WADC TECHNICAL REPORT 54-579

ANALYTICAL STUDIES
OF
AIRCRAFT STRUCTURES EXPOSED TO TRANSIENT EXTERNAL HEATING.

VOLUME II
THERMAL RESPONSE OF A FINITE PLATE
AND
THE "THIN" PLATE CRITERION

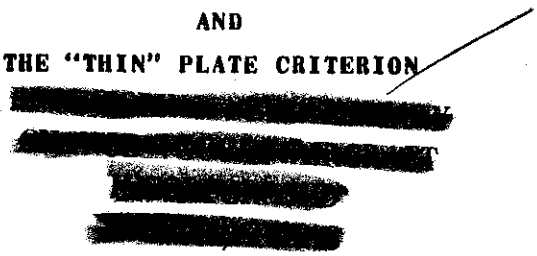

Alphonso Ambrosio
Takao Ishimoto

University of California
Department of Engineering
Los Angeles 24, California

November 1954

Aircraft Laboratory
Contract No. AF 33(616)-293
Project No. 1350

Wright Air Development Center
Air Research and Development Command
United States Air Force
Wright-Patterson Air Force Base, Ohio

FOREWORD

This report was prepared by A. Ambrosio and T. Ishimoto of the Department of Engineering, University of California, Los Angeles, under Contract No. AF 33(616)-293. The contract was initiated under Project No. 1350, "Effects of Atomic Weapons on Aircraft Systems," and was administered by the Aircraft Laboratory, Directorate of Laboratories, Wright Air Development Center, with Lt. Leonard C. Pincus acting as project engineer.

Alphonso Ambrosio directed and was technically responsible for the research described in this report and Walter C. Hurty acted as the representative of the Chairman of the Department, L.M.K. Boelter.

The authors wish to acknowledge the assistance given by R. Wagner and J. Schwartz in the preparation of this report.

ABSTRACT

This report is one of a series on analytical studies of aircraft structures exposed to transient external heating. In this study a criterion for predicting the maximum thickness of a "thin" skin that is thermally isolated from the supporting members is presented. The term "thin" states that the temperature difference across the skin is negligible compared to its maximum temperature rise. The criterion accounts for the effect of convective cooling and is established in terms of dimensionless parameters containing material properties and boundary conditions. The results are presented in graphical form.

PUBLICATION REVIEW

This report has been reviewed and is approved.

FOR THE COMMANDER:

for Carl A. Ruechardt

Daniel D. McKee
Colonel, USAF
Chief, Aircraft Laboratory
Directorate of Laboratories

CONTENTS

		Page
INTRODUCTION		1
SECTION I.	MATHEMATICAL MODEL OF PHYSICAL SYSTEM	3
SECTION II.	ANALYSIS OF MATHEMATICAL MODEL	9
SECTION III.	RESULTS	21
SECTION IV.	DISCUSSION AND SAMPLE USAGE OF RESULTS	29
SECTION V.	CONCLUSIONS	33
BIBLIOGRAPHY		35
APPENDIX A.	POLES OF THE TRANSFORMED SOLUTION	37
APPENDIX B.	A METHOD OF EVALUATING THE TEMPERATURE SOLUTION	43
APPENDIX C.	ISOLATED "THIN" PLATE SOLUTION	47

LIST OF FIGURES

Figure	Title	Page
1	The Physical System and Its Reduction to a Mathematical Model	4
2	The Transient Heating Function	5
3	Graphical Formulation of "Thin" Plate Criterion	17
4	Graphical Formulation of Minimum "Thin" Plate Criterion	19
5	"Thin" Plate Criterion with a 5% Temperature Ratio	22
6	"Thin" Plate Criterion with a 10% Temperature Ratio	23
7	"Thin" Plate Criterion with a 20% Temperature Ratio	24
8	Minimum "Thin" Plate Criterion (Independent of Time)	25
9	Simplified "Thin" Plate Criterion (Independent of Time & Bi/β) with a 5% Temperature Ratio	26
10	Simplified "Thin" Plate Criterion (Independent of Time & Bi/β) with a 10% Temperature Ratio	27
11	β_{min} versus Temperature Ratio	28
A-1	First of Two Graphs Showing Poles are Imaginary	39
A-2	Second of Two Graphs Showing Poles are Imaginary	41
A-3	A Plot of $Tan\ V = Bi/V$ $(Bi = 3)$	42
B-1	"Thin" Plate System with a Typical Graphical Presentation of Solution	45
C-1	Plot of Maximum "Thin" Skin Temperature Rise	48
C-2	Plot of Time to Maximum "Thin" Skin Temperature Rise	49

NOMENCLATURE

a	Thermal diffusivity	ft^2/hr
A	Area	ft^2
b	Thickness	ft
Bi	Biot's modulus $(h_c b/k)$	dimensionless
C_p	Heat capacity	Btu/lb °F
h	Unit thermal conductance	Btu/lb ft^2 °F
k	Thermal conductivity	Btu/hr ft^2(°F/ft)
q	Heat rate per unit area	Btu/hr ft^2
Q	Total heat $\left(\int_0^\infty q(t)dt\right)$	Btu/ft^2
s	Variable of Laplace transformation	Sec^{-1} or hr^{-1}
t	Elapsed time	Sec or hr
T	Temperature	°F or °R
y	Distance	ft
Y	Dimensionless quantity (y/b)	
I	Integral	dimensionless
β	Dimensionless quantity $(b/\sqrt{a\eta})$	
γ	Density	lb/ft^3
Δ	Difference	
η	Reference time	sec or hr
τ	Dimensionless quantity $(h_c \eta/\gamma C_p b)$	

SUBSCRIPT

c	convective	m	maximum
ref	reference	min	minimum
∞	ambient	o	initial
$T.P.$	"Thin" Plate		

SUPERSCRIPT

+	dimensionless quantity

INTRODUCTION

When an aircraft is exposed to transient external heating and convective cooling, the outer skin undergoes a temperature rise that varies along the chord, the span, and across the thickness of the skin. Because the temperature distributions of this system cannot be obtained readily, they are approximated with the aid of unidimensional models.

Of these models the one that is used to approximate the temperature distribution across the thickness of the skin is of considerable interest. If the temperature expression of this model is presented as a ratio of temperature drop (front surface temperature minus the back surface temperature) to a reference temperature, conditions exist under which this temperature ratio is small. By specifying an allowable value for this ratio, a criterion that predicts the temperature invariancy across the skin can be established in terms of the boundary conditions and the material properties of the system.

A similar mathematical model was previously analyzed;[1*] however, that study considered only the effect of the heating function. The present study includes the effect of convective cooling but only one particular heating function.

The thermal analysis of the outer skin of an aircraft is considerably simplified by the use of this criterion which is termed a "Thin" Plate Criterion.

*Superscript numbers indicate references listed at the end of this report.

SECTION I
MATHEMATICAL MODEL OF PHYSICAL SYSTEM

Physical System

A section of the type of aircraft structures which are under consideration in this report is illustrated in Figure 1. The lower surface of the skin is exposed to an external heat source and to forced convection. In addition to convective cooling from the outer surface, heat is also lost by radiation. The predominant mode of heat transfer on the upper surface is free convection.

Heat Source

The transient heating function (Figure 2) is not denoted mathematically but is identified as a curve having a sharp rise at the outset of the function and a moderate slope at longer periods. The reference time, η , defined as the elapsed time to the peak input is incorporated in the dimensionless parameter, τ, as well as the dimensionless time, t^+.

Convective Cooling

Forced convective cooling resulting from the flow of fluid over a heated surface is denoted by the unit thermal conductance, h_c. Equations predicting these conductances over isothermal and non-isothermal surfaces are available.[2,3,5,6]

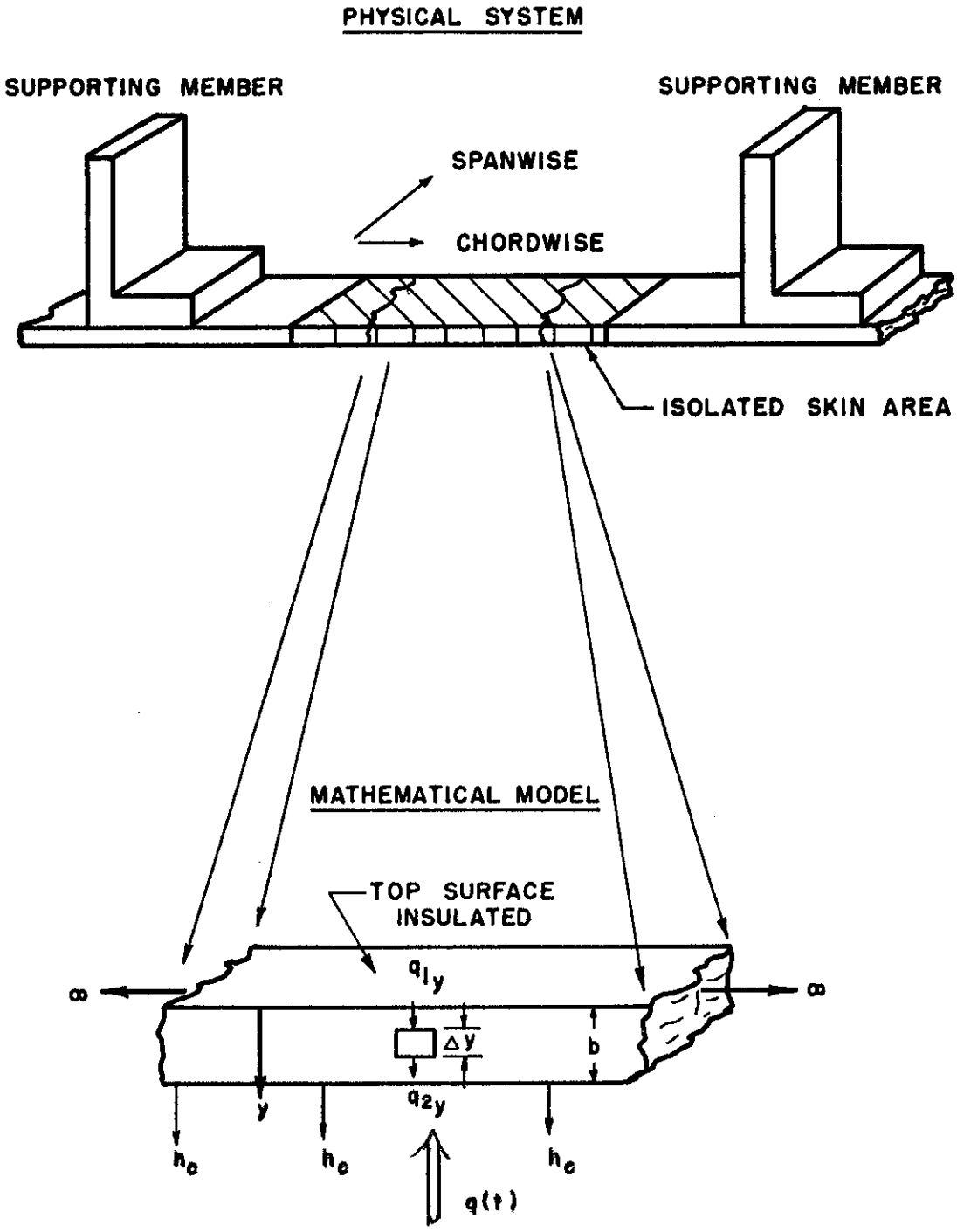

FIGURE 1 THE PHYSICAL SYSTEM AND ITS REDUCTION TO A MATHEMATICAL MODEL

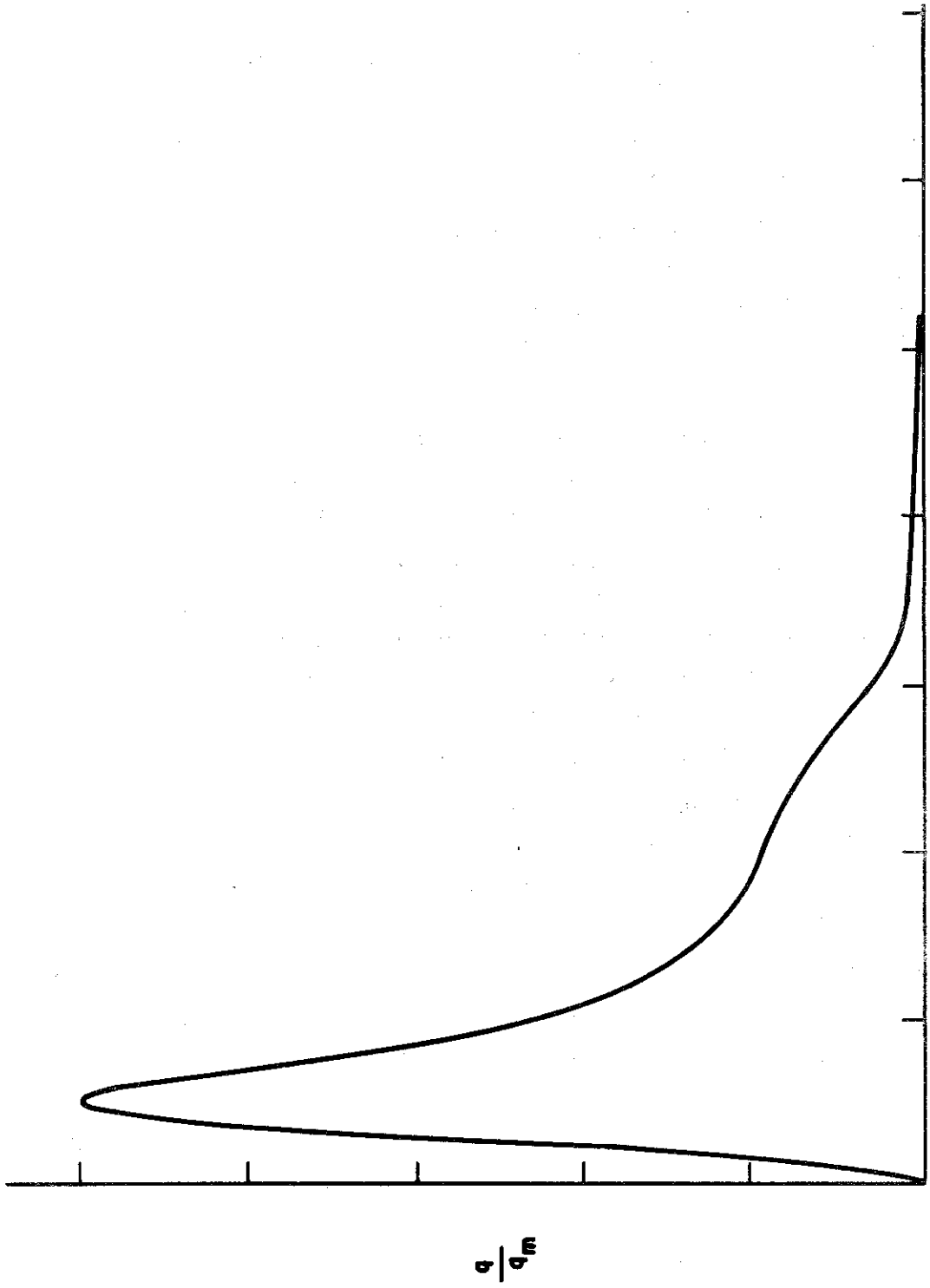

FIGURE 2 THE TRANSIENT HEATING FUNCTION

Mathematical Model

The outer skin of the structure illustrated in Figure 1 may be separated into three idealized thermal regions:

(1) The skin region beneath the stringer;

(2) The skin region (adjacent to the stringer) that is thermally influenced by the stringer; and

(3) The skin region that is thermally isolated from the supporting member.

The present study is concerned only with the thermal behavior of region (3). A discussion of the criterion for the determination of thermally isolated areas is given in reference[4]. Region (3) is reduced to the unidimensional model (illustrated in Figure 1) by the following postulations:

(1) The inner (back) surface of the skin is insulated. The inner surface loses heat by free convection but its magnitude is small compared to forced convective cooling.[2]

(2) The unit thermal conductance is constant and uniform along the chordwise length of the wing. In reality, the skin undergoes a nonuniform temperature rise resulting in nonuniform unit thermal conductances. Unit thermal conductances are discussed in several references.[2,3,5,6]

(3) The material properties are independent of temperature.

(4) Radiation losses from the airfoil are small compared to forced convection heat losses.[2]

(5) Temperature along the direction of the chord is nonvariant.

(6) The initial temperature is the ambient air temperature.

The differential equation of the mathematical model is derived by taking a heat balance on an element of length Δy in the skin (Figure 1).

In the y-direction

The heat flow **in** is:

$$q_{1_y} = -k\,Ay\,\frac{\partial(T - T_\infty)}{\partial y} \tag{1a}$$

The heat flow **out** is:

$$q_{2_y} = -k\,A_y\,\frac{\partial}{\partial y}\left[(T - T_\infty) + \frac{\partial}{\partial y}\,(T - T_\infty)\,\Delta y\right] \tag{1b}$$

Heat Stored

$$q_s = \gamma C_p A_y \Delta y\,\frac{\partial}{\partial t}(T - T_\infty) \tag{1c}$$

Equate the heat flow **in** to the sum of the heat flow **out** and the heat stored.

$$-k\,A_y\,\frac{\partial}{\partial y}(T - T_\infty) = -k\,A_y\,\frac{\partial}{\partial y}\left[(T - T_\infty) + \frac{\partial}{\partial y}(T - T_\infty)\Delta y\right]$$

$$+\ \gamma\,C_p\,A_y\,\Delta y\ \frac{\partial}{\partial t}(T - T_\infty)$$

or:

$$k\,\frac{\partial^2}{\partial y^2}(T - T_\infty) = \gamma C_p\,\frac{\partial}{\partial t}(T - T_\infty) \tag{3}$$

The boundary and initial conditions for the model are:

$$\text{at} \quad y = 0, \qquad k\,\frac{\partial(T - T_\infty)}{\partial y} = 0 \tag{4a}$$

at $y = b$, $k\frac{\partial(T - T_\infty)}{\partial y} = q(t) - h_c(T - T_\infty)$; (4b)

and when $t = 0$, $T(y, 0) = T_\infty$; (4c)

where

k = thermal conductivity (Btu/hr, ft^2, °F/ft)

T = temperature (°F)

y = distance from insulated surface (ft)

T_∞ = ambient temperature (°F)

C_p = heat capacity (Btu/lb, °F)

γ = density of plate (lb/ft^3)

t = time (hr)

b = skin thickness (ft)

$q(t)$ = heating function (Btu/hr, ft^2)

h_c = unit thermal conductance (Btu/hr, ft^2, °F)

A_y = elemental area normal to the direction of heat flow, (ft^2)

SECTION II
ANALYSIS OF MATHEMATICAL MODEL

The expression for the temperature distribution through the thickness of the skin may be found by solving equation (3) with the prescribed initial and boundary conditions (4a, 4b, and 4c); but it is more convenient to present the differential equation of the model in a dimensionless form. The temperature response of the skin is then specified in terms of dimensionless quantities incorporating boundary conditions and material properties. These quantities, in turn, are used to establish a criterion for predicting the temperature invariancy across the skin thickness.

By rearranging and manipulating the terms in equation (3), the heat conduction equation is expressed in the following dimensionless form:

$$\frac{\partial^2 T^+}{\partial Y^2} = \beta^2 \frac{\partial T^+}{\partial t^+} \tag{5}$$

The initial and boundary conditions are expressed as follows:

when $t^+ = 0, \quad T^+ = 0;$ (6a)

at $Y = 0, \quad \frac{\partial T^+}{\partial Y} = 0;$ (6b)

and at $Y = 1, \quad \frac{1}{\beta^2} \frac{\partial T^+}{\partial Y} = \frac{q^+(t^+)}{I} - \tau T^+$ (6c)

where:

$$T^+ = \frac{T - T_\infty}{\Delta T_{ref}} \left(\Delta T_{ref} = \frac{Q}{\gamma C_p b} \right)$$

$$Y = y/b$$

$$t^+ = t/\eta$$

$$\beta = b/\sqrt{a\eta}$$

$$q^+(t^+) = q/q_m$$

$$\tau = h_c \eta/\gamma C_p b$$

$$I = \int_0^\infty q^+(t^+)dt^+$$

The Laplace transformation of equation (5) with respect to the time variable yields an ordinary differential equation,

$$\frac{d^2T^+(Y,s)}{dY^2} = \beta^2 sT^+(Y,s) \tag{7}$$

with the following transformed boundary conditions:

$$\text{at } Y = 0, \quad \frac{dT^+(Y,s)}{dY} = 0 \tag{8a}$$

$$\text{and at } Y = 1, \quad \frac{dT^+(Y,s)}{dY} = \frac{q^+(s)}{I} - \tau T^+(Y,s); \tag{8b}$$

the complex variable of Laplace transformation is denoted by s.

The solution of equation (7) is written in terms of hyperbolic functions,

$$T^+(Y,s) = A \cosh \sqrt{s}\,\beta Y + B \sinh \sqrt{s}\,\beta Y, \tag{9}$$

with constants A and B that are evaluated from boundary conditions (8a) and (8b).

From condition (8a),

$$\left\{\frac{dT^+(Y,s)}{dY}\right\}_{Y=0} = \sqrt{s}\,\beta \left\{(A \sinh \sqrt{s}\,\beta Y) + B \cosh\sqrt{s}\,\beta Y\right\}_{Y=0} = 0 \tag{10}$$

Equation (10) is true only if B is zero.

The constant A is evaluated from the boundary condition at $Y = 1$.

$$\frac{\sqrt{s}}{\beta^2}\beta A \sinh\sqrt{s}\,\beta = \frac{q^+(s)}{I} - \tau A \cosh\sqrt{s}\,\beta$$

or:

$$A = \frac{q^+(s)}{I}\frac{1}{\left[\frac{\sqrt{s}}{\beta}\sinh\sqrt{s}\,\beta + \tau\cosh\sqrt{s}\,\beta\right]} \tag{11}$$

Thus, the transformed solution of equations (5) and (6) is,

$$T^+(Y,s) = \frac{q^+(s)}{I}\left[\frac{\cosh\sqrt{s}\,\beta Y}{\left[\frac{\sqrt{s}}{\beta}\sinh\sqrt{s}\,\beta + \tau\cosh\sqrt{s}\,\beta\right]}\right] \tag{12}$$

Because the forcing function, $q^+(t^+)/I$ is not identified mathematically, the inverse transformation is written as a convolution of two functions; the convolution is denoted symbolically by the star, *.

$$T^+(Y,t^+) = F_1 * F_2 \tag{13}$$

where:

$$F_1 = \frac{q^+(t^+)}{I}$$

$$F_2 = \mathcal{L}^{-1}\left\{\frac{\cosh\sqrt{s}\,\beta Y}{\left[\frac{\sqrt{s}}{\beta}\sinh\sqrt{s}\,\beta + \tau\cosh\sqrt{s}\,\beta\right]}\right\}$$

The system function containing the ratio of hyperbolic functions is inverted by representing the inverse transformation by a series of residues. Because the system function has the fractional form, $p(s)/r(s)$,

where $p(s)$ and $r(s)$ are analytic at $s = s_n$ and $p(s_n) = 0$, the residue at the simple pole, s_n, is

$$\frac{p(s_n)\ e^{s_n t^+}}{r'(s_n)} \tag{14}$$

where: $p(s_n) = \cosh\sqrt{s_n}\beta Y,$

$$r(s_n) = \frac{\sqrt{s_n}}{\beta} \sinh\sqrt{s_n}\,\beta + \tau\cosh\sqrt{s_n}\,\beta$$

and $r'(s_n)$ is the derivative of $r(s)$ with respect to s and evaluated at s_n. Hence,

$$r'(s_n) = \frac{1}{2}\left[\left(\frac{1}{\sqrt{s}\,\beta} + \frac{\tau\beta}{\sqrt{s}}\right) \sinh\sqrt{s_n}\beta + \cosh\sqrt{s_n}\beta\right]$$

Thus, F_2 is represented by the following series,

$$F_2 = \sum_{n=1}^{\infty} \frac{p(s_n)e^{s_n t^+}}{r'(s_n)} \tag{15}$$

where the poles, s_n, are the roots of $r(s)$. By equating $r(s)$ to zero, the following equation is obtained:

$$\frac{\sqrt{s}}{\beta}\sinh\sqrt{s}\,\beta + \tau\cosh\sqrt{s}\,\beta = 0 \tag{16}$$

Changing variables,

$$\alpha \sinh\alpha + Bi\cosh\alpha = 0 \tag{17}$$

where: $\alpha = \sqrt{s}\,\beta$ and $Bi = \tau\beta^2$

$\alpha = U + iV$

The real part (U) of α is zero (refer to Appendix A for this proof), so that equation (16) reduces to the expression,

$$\tan \nabla = Bi/\nabla \tag{18}$$

The values of $\nabla_n = \nabla_1, \nabla_2 \ldots\ldots$ that satisfy equation (18) are known as eigenvalues and may be found graphically as shown in Appendix A. Because the square root of the simple pole, s_n, is an imaginary quantity,

$$\sqrt{s_n} = i(\nabla_n/\beta) \ , \ (\nabla_n \text{ is both positive and negative}) \tag{19}$$

the simple poles are all negative.

By using equations (14), (15), and (19) to evaluate F_2 and substituting this into equation (13), the expression for the temperature response of a finite plate becomes,

$$T^+(Y, t^+) = \frac{q^+(t^+)}{I} * \sum_{n=1}^{\infty} \frac{\cosh(i\nabla_n Y) \exp\left[-(\nabla_n^2/\beta^2)\, t^+\right]}{\tfrac{1}{2}\left[\cosh(i\nabla_n) + \left(\frac{1}{i\nabla_n} + \frac{Bi}{i\nabla_n}\right)\sinh(i\nabla_n)\right]} \tag{20}$$

But,

$$\cosh(i\nabla_n Y) = \cos(\nabla_n Y) \tag{21}$$

and

$$\sinh(i\nabla_n Y) = i \sin(\nabla_n Y)$$

Thus equation (20) is written as

$$T^+(Y,t^+) = \frac{q^+(t^+)}{I} * \sum_{n=1}^{\infty} 2\,\frac{\cos(V_n Y)\exp[-V_n^2/\beta^2)t^+]}{\left[\cos V_n + \left(\frac{1}{V_n} + \frac{Bi}{V_n}\right)\sin V_n\right]} \qquad (22)$$

But from equation (18), $\cos V_n = \frac{V_n}{Bi}\sin V_n$, thus equation (22) can also be written as

$$T^+(Y,t^+) = \frac{q^+(t^+)}{I} * \sum_{n=1}^{\infty} \frac{2\cos(V_n Y)\exp\left[-(V_n^2/\beta^2)t^+\right]}{\cos V_n\left[1 + \frac{Bi}{V_n^2}(1 + Bi)\right]} \qquad (23)$$

The expressions for the front and back surface temperatures of the plate are taken directly from equation (23) by substituting appropriate values of Y.

The temperature rise at the front surface, $Y = 1$, (heated surface) is

$$T^+(1,t^+) = \frac{q^+(t^+)}{I} * \sum_{n=1}^{\infty} \frac{2\exp\left[-(V_n^2/\beta^2)t^+\right]}{\left[1 + \frac{Bi}{V_n^2}(1 + Bi)\right]} \qquad (24)$$

At the back surface, $Y = 0$, (insulated surface), the temperature rise is:

$$T^+(0,t^+) = \frac{q^+(t^+)}{I} * \sum_{n=1}^{\infty} \frac{2\exp[-(V_n^2/\beta^2)t^+]}{\cos V_n\left[1 + \frac{Bi}{V_n^2}(1 + Bi)\right]} \qquad (25)$$

The temperature difference between the front and back surfaces is found by subtracting equation (25) from equation (24).

$$T^+(1,t^+) - T^+(0,t^+) = \frac{q^+(t^+)}{I} * \sum_{n=1}^{\infty} \frac{2(\cos V_n - 1)\exp[-(V_n^2/\beta^2)t^+]}{\cos V_n\left[1 + \frac{Bi}{V_n^2}(1 + Bi)\right]} \qquad (26)$$

Establishment of the "Thin" Plate Criteria

The "thin" plate criterion is used for the specific purpose of predicting skin thickness that satisfies the condition of negligible temperature drop across the skin as compared to a suitable reference temperature. This criterion is specified in terms of the following quantities:

(1) The ratio of temperature difference across the skin to reference temperature;

(2) Material properties and boundary conditions (these are incorporated in the dimensionless parameters, τ and β);

(3) Elapsed time.

Of these quantities, only the reference temperature has not been defined. A suitable reference temperature for this criterion is the maximum temperature rise of the skin when the skin is considered "thin". A discussion of maximum "thin" skin temperature rise is found in references 3 and 4. In dimensionless form, this maximum "thin" skin temperature rise, $T^{+}_{m(T.P.)}$ is

$$T^{+}_{m(T.P.)} = \frac{T_{m(T.P.)} - T_{\infty}}{\Delta T_{ref}} \tag{27}$$

where ΔT_{ref} is defined as the maximum possible temperature rise of a "thin" plate, $\Delta T_{ref} = Q/\gamma C_p b$, i.e., ΔT_{ref} is the temperature rise of a "thin" plate if there were no convective heat loss.

Dividing equation (26) (the expression for the dimensionless temperature difference across the skin) by this maximum "thin" skin temperature rise results in

$$\frac{T^{+}(1,t^{+}) - T^{+}(0,t^{+})}{T^{+}_{m(T.P.)}} \equiv \frac{\Delta T^{+}}{T^{+}_{m(T.P.)}}$$

$$= \frac{\dfrac{q^{+}(t^{+})}{I} * \displaystyle\sum_{n=1}^{\infty} \frac{2\ (\cos V_n - 1)\exp[-(V_n^2/\beta^2)\ t^{+}]}{\cos V_n \left[1 + \dfrac{Bi}{V_n^2}\ (1 + Bi)\right]}}{T^{+}_{m(T.P.)}} \tag{28}$$

or

$$\frac{\Delta T^+}{T^+_{m(T.P.)}} = \frac{2\int_0^{t^+} \frac{q^+(\lambda)}{I} \sum_{n=1}^{\infty} \frac{(\cos V_n - 1)\ exp\left[-\frac{V_n^2}{\beta^2}(t^+ - \lambda)\right]}{\cos V_n \left[1 + \frac{Bi}{V_n^2}(1 + Bi)\right]} d\lambda}{T^+_{m(T.P.)}} \tag{29}$$

The temperature ratio expressed in equation (29) was evaluated numerically by a method that is essentially a superposition technique. This method is discussed in Appendix B.

Time Dependent "Thin" Plate Criterion

The results of this numerical evaluation were plotted in terms of temperature ratio, $\Delta T^+/T^+_{m(T.P.)}$ versus time, t^+. For each set of curves, β was used as a parameter and Biot's Modulus, Bi, was held constant. A typical set of curves is illustrated in Figure (3a). As an intermediate step toward obtaining the curves which establish the "thin" plate criterion, the curves illustrated in Figure (3a) were cross-plotted in terms of temperature ratio versus Bi/β. Bi was used as a parameter and elapsed time was held constant for each set of curves as illustrated in Figure (3b). The final curves were obtained by cross-plotting the intermediate curves. In this cross-plot, the temperature ratio was held constant, the elapsed time was considered as the parameter, and β was plotted versus Bi/β.

These final curves may be used directly to determine the maximum thickness of a plate which may be considered "thin" because the independent variable for these curves, Bi/β, is not a function of plate thickness. The quantity Bi/β is determined from the material properties, the thermal conductance, and the time to peak input. Use of these curves to determine maximum plate thickness of a "thin" plate is illustrated in Section IV.

Time Independent "Thin" Plate Criterion

The curves discussed above specify the "thin" plate criterion in terms of elapsed time. A more conservative criterion, i.e., one that results in smaller values of plate thickness, was obtained by considering only the maximum values of the temperature ratios. As a consequence, the resulting curves are

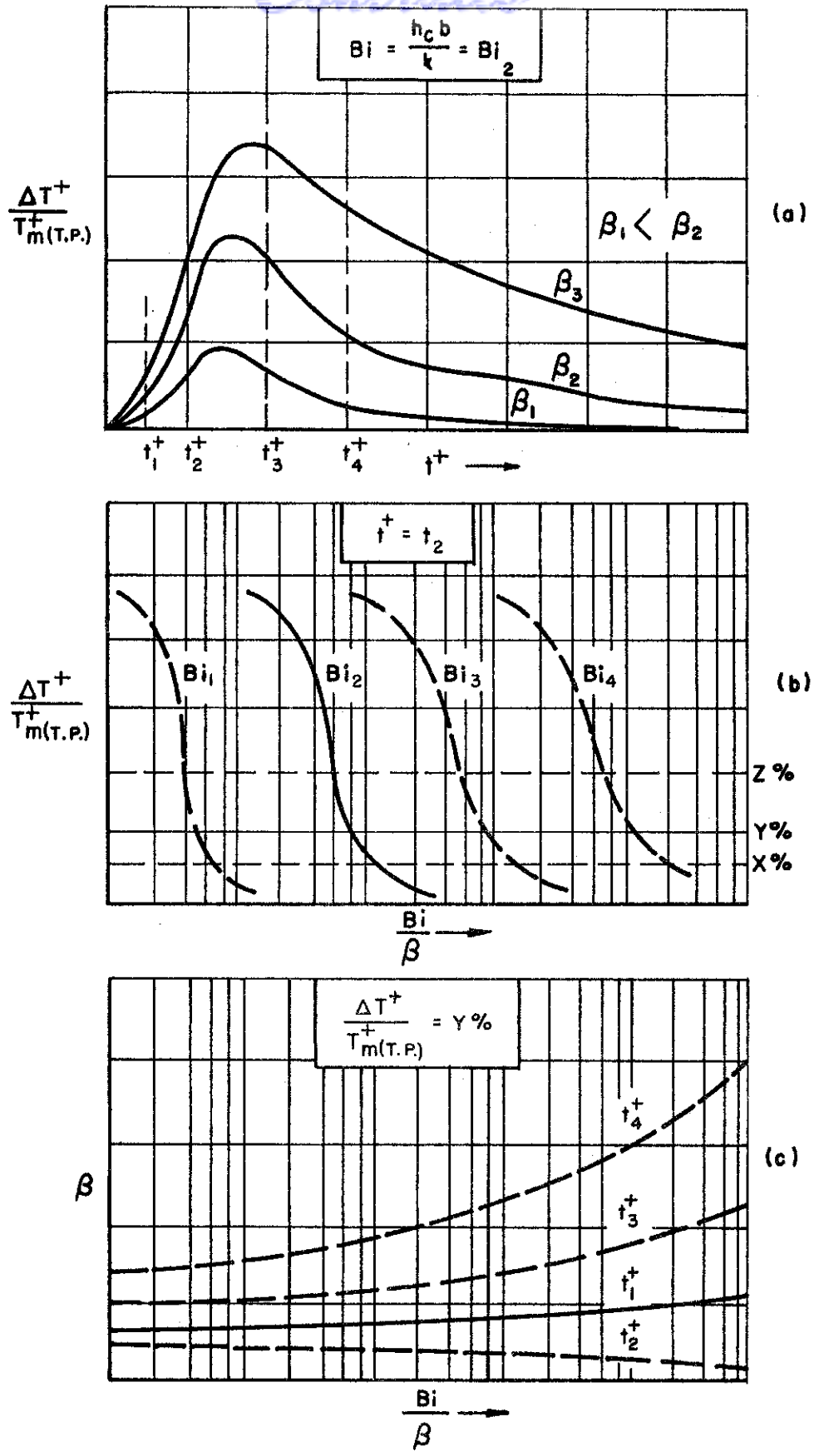

FIGURE 3 GRAPHICAL FORMULATION OF "THIN" PLATE CRITERION

independent of elapsed time. The method of cross-plotting used to obtain these curves is illustrated in Figures (4a), (4b), and (4c).

Simplified "Thin" Plate Criterion

The "thin" plate criterion may be further simplified by considering the time independent criterion to be independent of Bi/β. In the range of Bi/β considered, β varies approximately 30%; however, using the minimum value of β for each specified temperature ratio results in the most conservative "thin" plate criterion that is still realistic. With this approximation, an expression that predicts the thickness of the "thin" plate can be written as follows:

$$b = \sqrt{a\eta}\ \beta_{min} \tag{30}$$

where b = the thickness of the "thin" plate (ft),

a = the thermal diffusivity (ft^2/hr),

η = reference time or time to peak input (hr), and

β_{min} = minimum value of β for the specified temperature ratio.

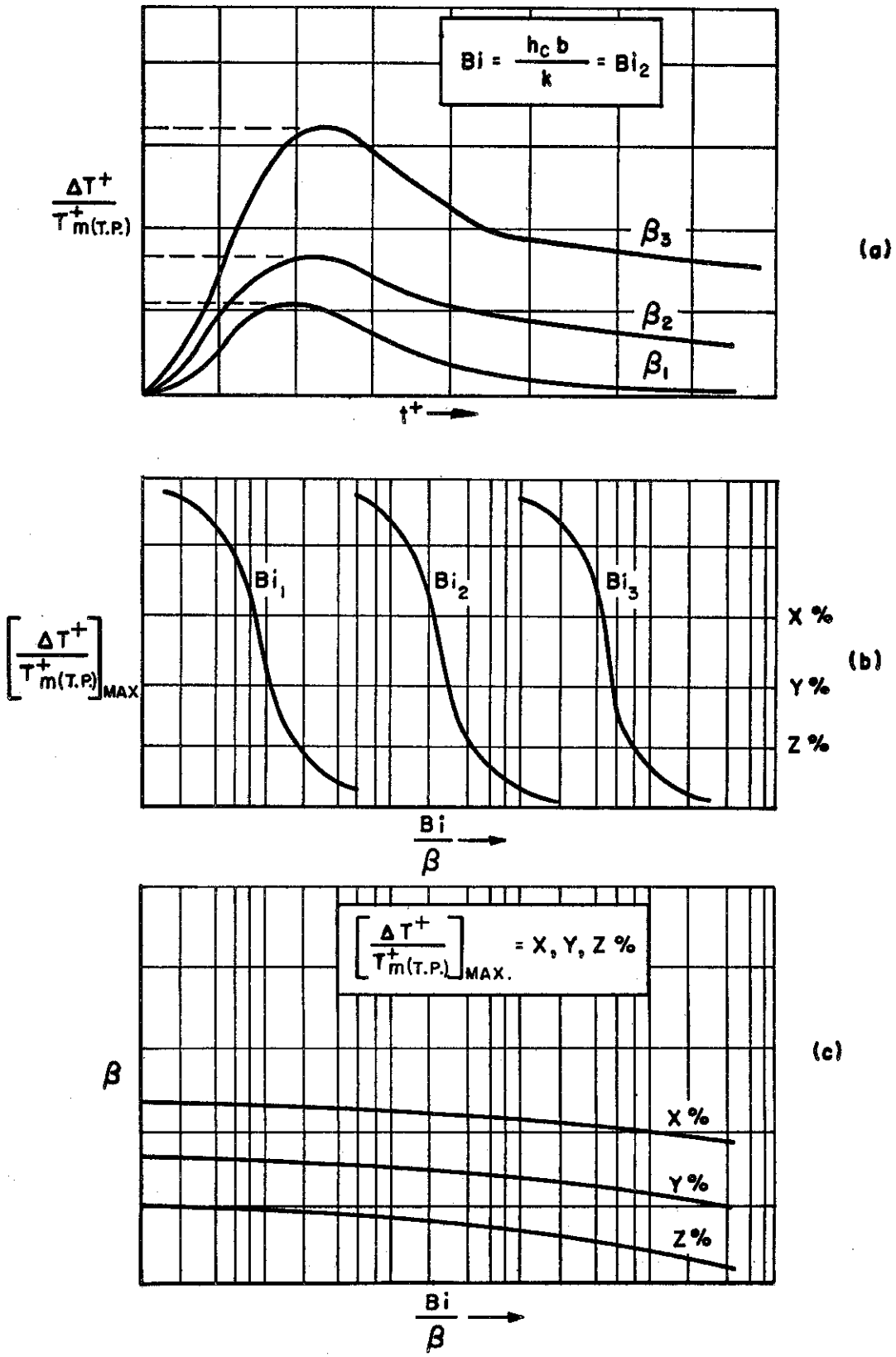

FIGURE 4 GRAPHICAL FORMULATION OF MINIMUM "THIN" PLATE CRITERION

SECTION III

RESULTS

The temperature ratio as expressed by equation (29) was evaluated and plotted for values of τ ranging from 0 to 10 and β from 0 to 25. The series of cross-plots discussed in Section II resulted in a set of curves for the "thin" plate criterion. These results are presented in Figures 5 through 8.

Figures 5 through 7 present β as a function of Bi/β with elapsed time, t^+, as a parameter. Each figure contains a set of curves for a specific temperature ratio as listed below.

$\Delta T^+/T^+_{m(F.P.)}$	*Figure Number*
5%	5
10%	6
20%	7

Figure 8 presents curves for the more conservative "thin" plate criterion. This criterion is not a function of elapsed time. Each curve in Figure 8 is for a specific temperature ratio.

Curves of equation (30), the simplified "thin" plate criterion, are presented in Figures 9 and 10 for temperature ratios, 5% and 10% respectively. These curves of "thin" plate thickness, b, versus reference time, η, have been plotted on a logarithmic scale using thermal diffusivity, a, as a parameter. Curves for pure magnesium, aluminum, pure titanium, and porcelain are included in these figures to indicate the magnitudes of "thin" plate thicknesses for a variety of materials.

Figure 11 presents a curve of β_{min} versus temperature ratio. This figure may be used in conjunction with equation (30) to determine a "thin" plate thickness at a temperature ratio other than those used in Figures 9 and 10.

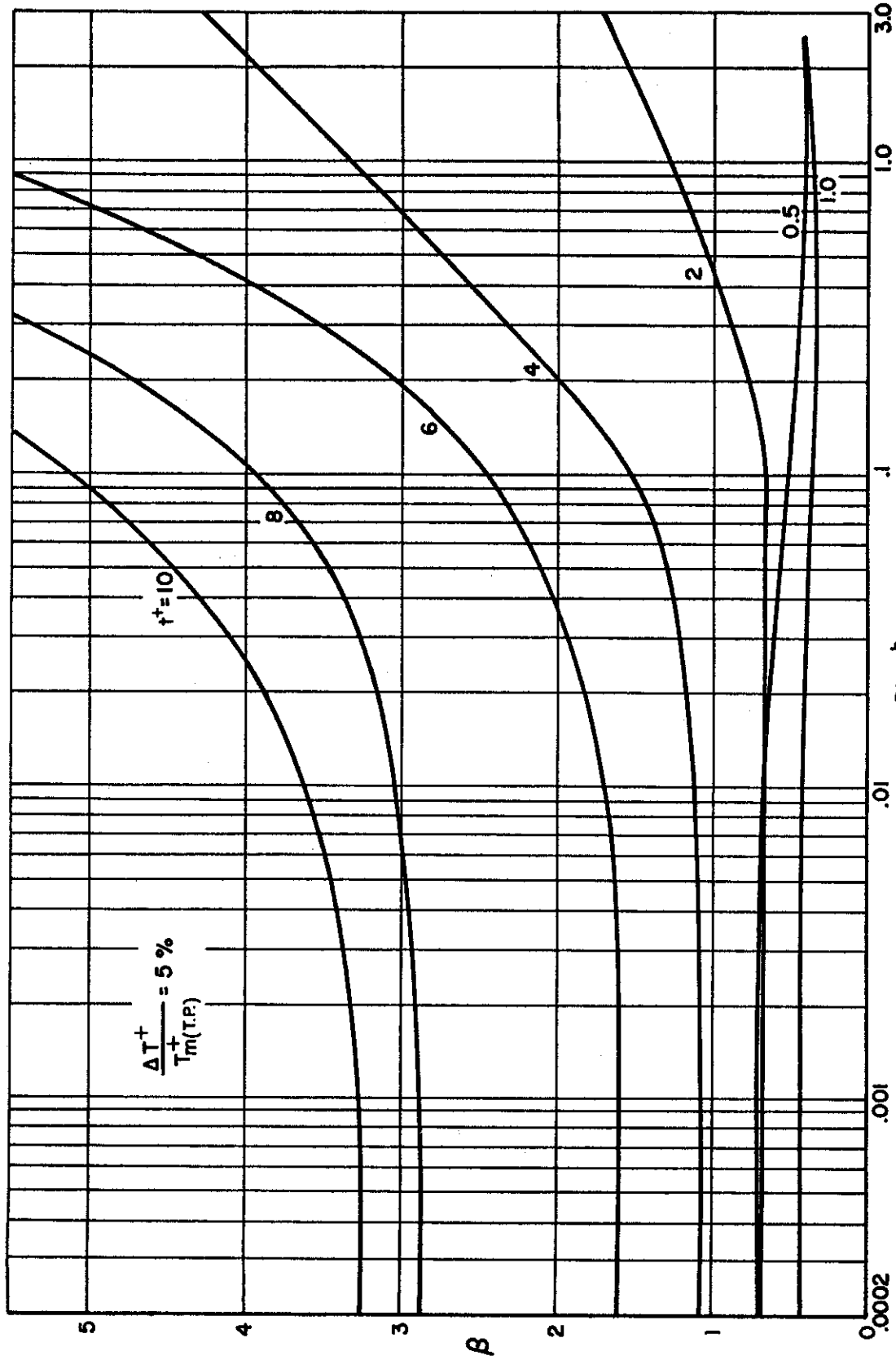

FIGURE 5 "THIN" PLATE CRITERION WITH A 5% TEMPERATURE RATIO

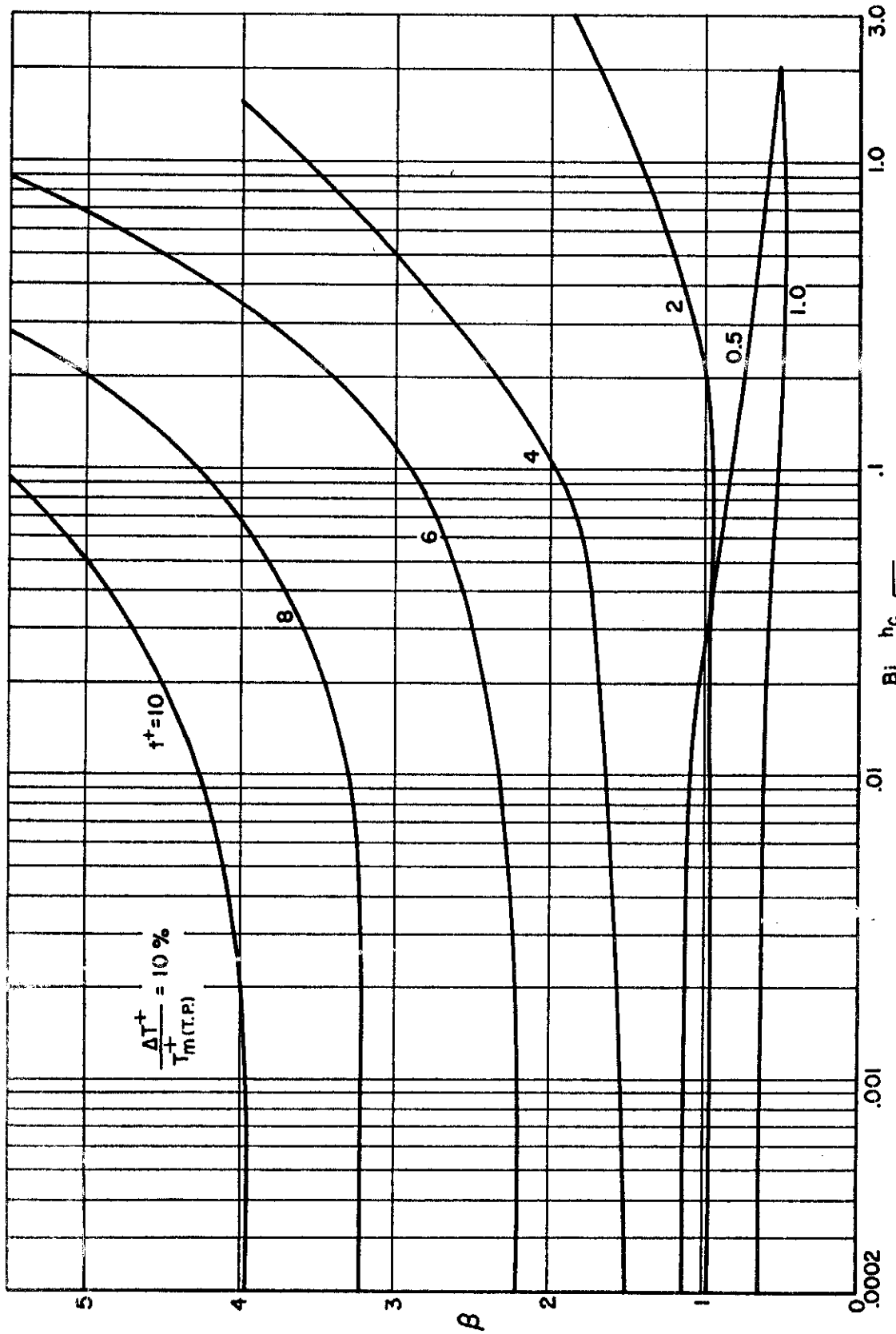

FIGURE 6 "THIN" PLATE CRITERION WITH A 10% TEMPERATURE RATIO

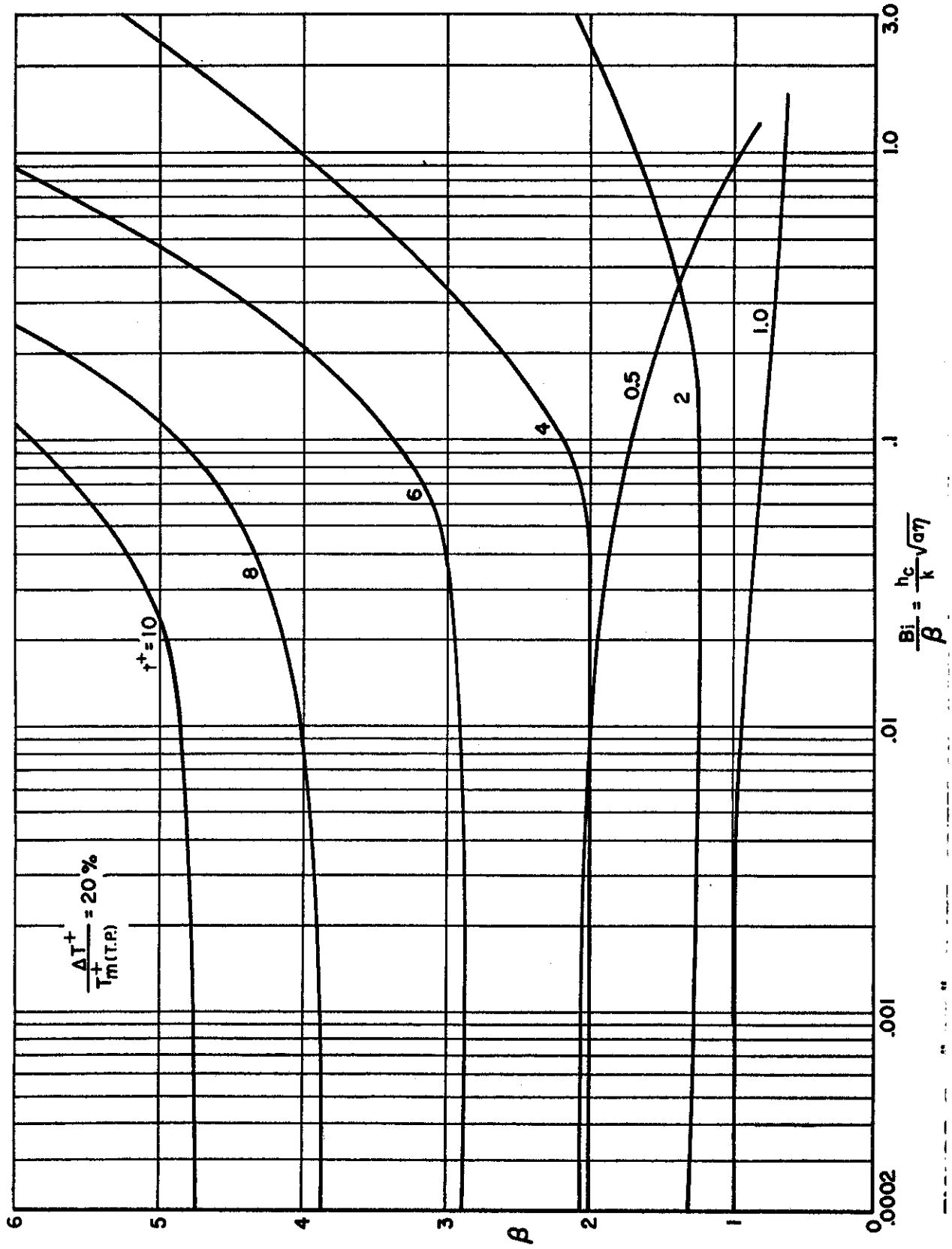

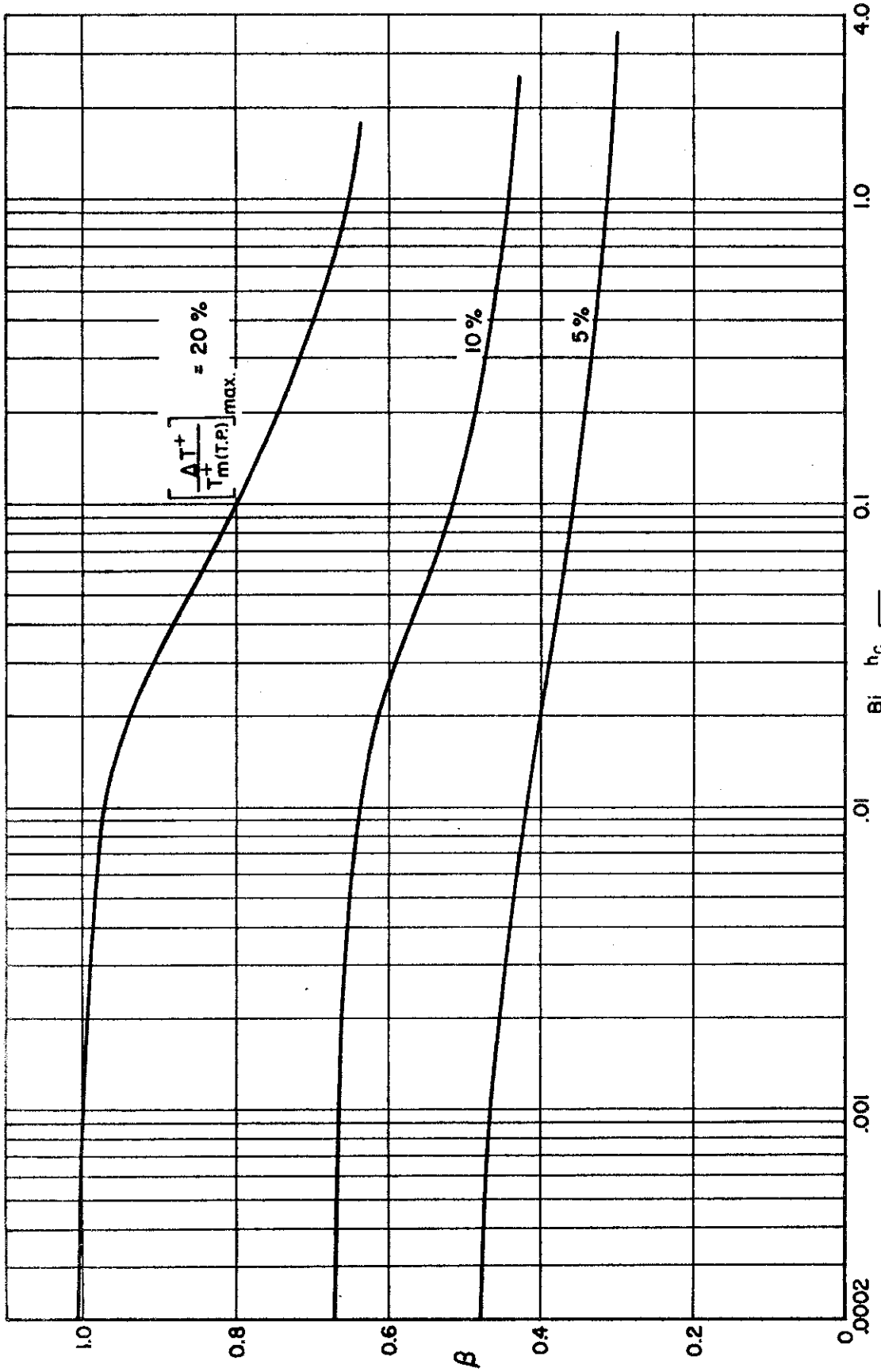

FIGURE 8 MINIMUM "THIN" PLATE CRITERION (INDEPENDENT OF TIME)

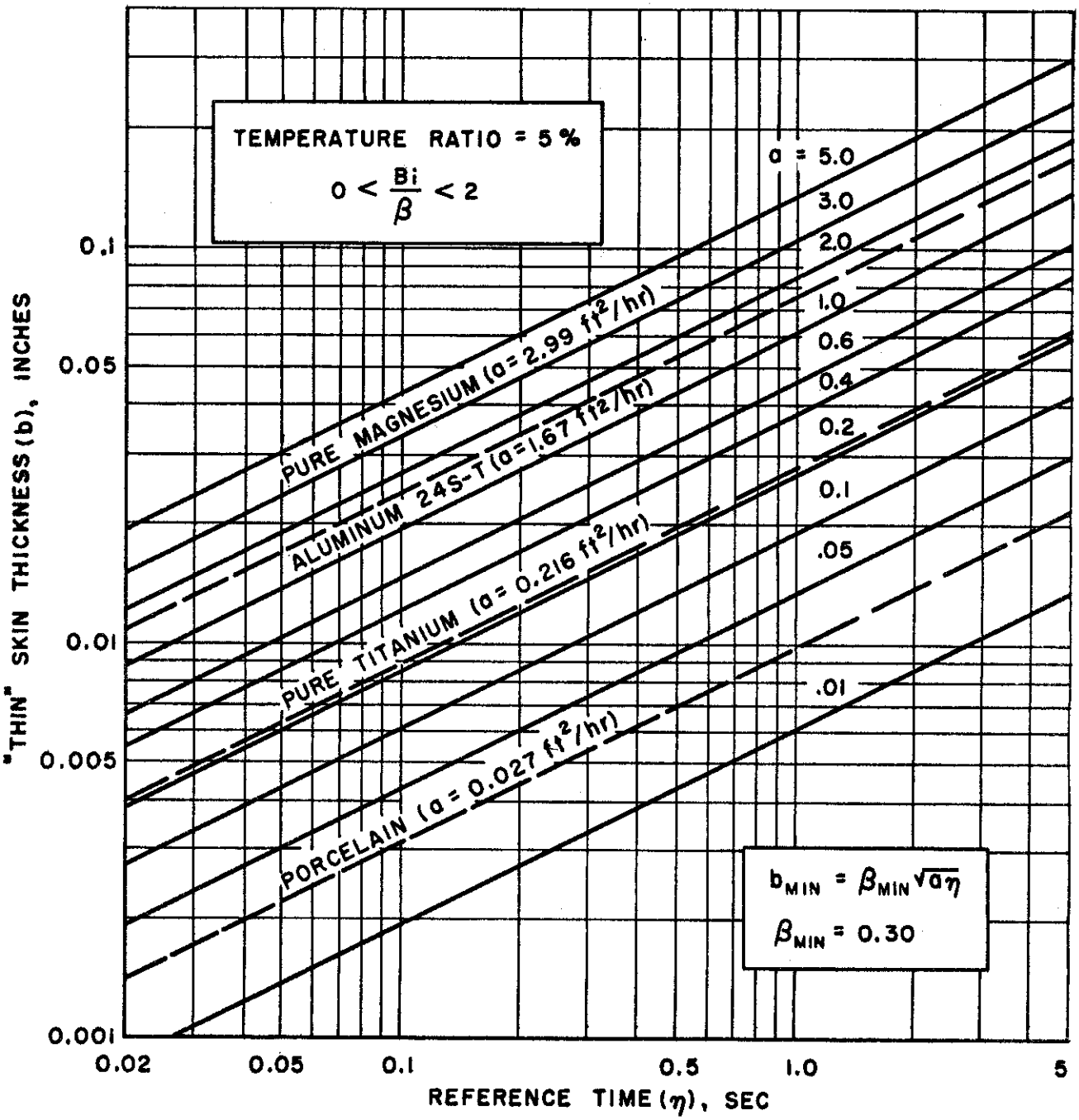

FIGURE 9 SIMPLIFIED "THIN" PLATE CRITERION (INDEPENDENT OF TIME AND Bi/β) WITH A 5% TEMPERATURE RATIO

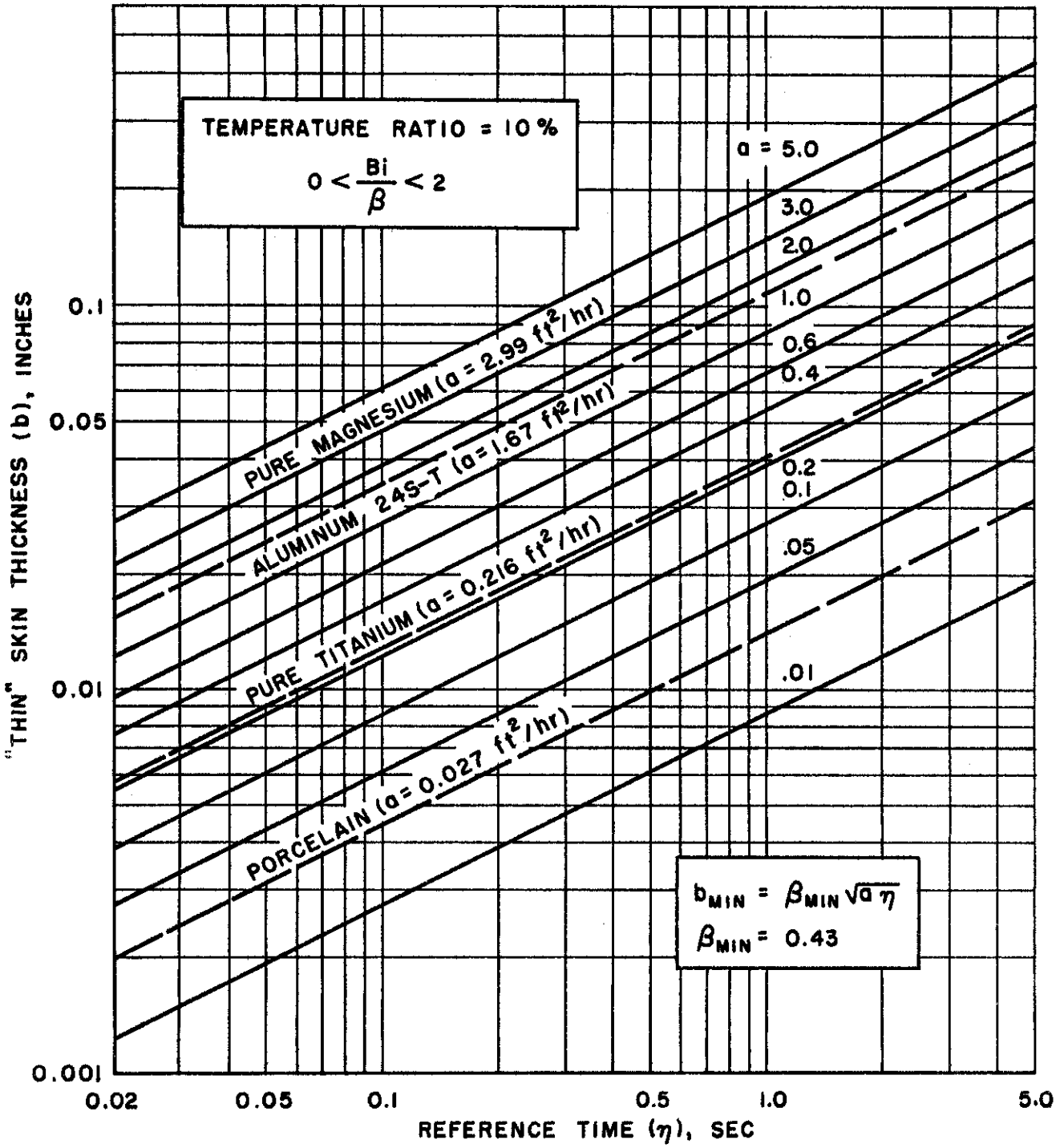

FIGURE 10 SIMPLIFIED "THIN" PLATE CRITERION (INDEPENDENT OF TIME AND Bi/β) WITH A 10% TEMPERATURE RATIO

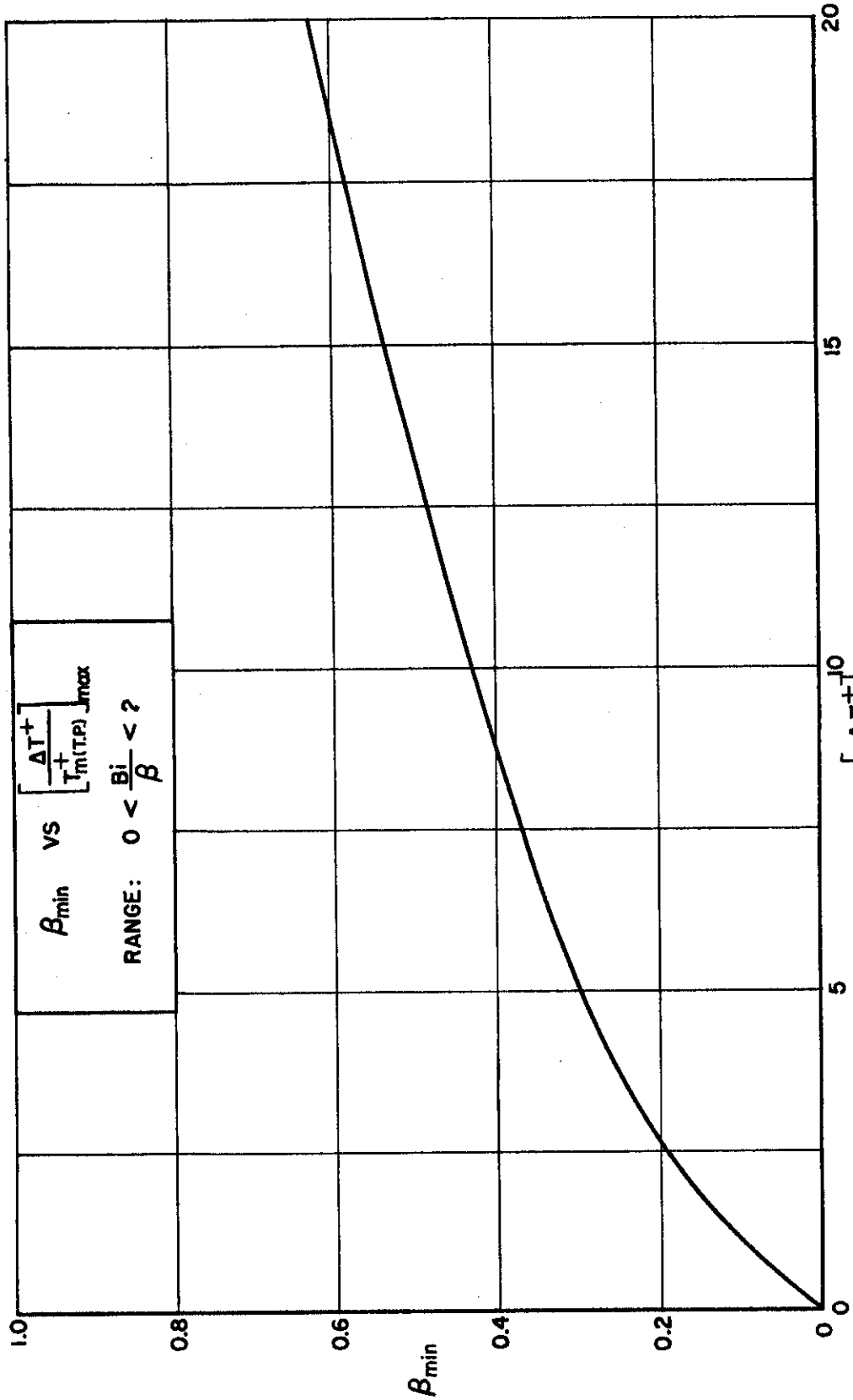

FIGURE 11 β_{min} VERSUS TEMPERATURE

SECTION IV

DISCUSSION AND SAMPLE USAGE OF RESULTS

The prediction of skin thicknesses that may be considered "thin" for the purpose of computing temperature distributions in a structure may be made by using one of the following set of curves, Figures 5 through 7, Figure 8, Figures 9 and 10, or Figure 11 in conjunction with equation (30).

The difference in the set of curves is the number of dimensionless parameters that specify the results; the use of fewer parameters gives more conservative (smaller skin thickness) results. To illustrate the use of each set in predicting a "thin" skin thickness, consider a 0.03 in. aluminum alloy 24S-T structure, similar to that shown in Figure 1. Consider, also, that the unit thermal conductance, h_c, on the surface of this structure is 25 Btu/hr ft^2 °F and that the time to the peak, η, of the thermal input is 3/3600 hr. In addition to these two quantities, the maximum allowable temperature ratio, $\Delta T^+/T^+_{m(T.P.)}$ is specified as 5%.

Because the quantity, Bi/β, is necessary in each set, it will simplify the presentation of the illustrations in each set by evaluating this term beforehand. This quantity, Bi/β, is defined as

$$Bi/\beta = h_c\sqrt{a\eta}/k$$

where:
- h_c = 25 Btu/hr ft^2°F (unit thermal conductance)
- η = 3/3600 hr (reference time)
- k = 66.7 Btu/hr ft^2°F/ft (thermal conductivity of structure)
- a = 1.68 ft^2/hr (thermal diffusivity of structure)

Thus: Bi/β = 0.014 (dimensionless)

This value is utilized consistently in the examples to follow.

Set I. Figures 5 through 7.

The variation of skin thickness (included in β) with convective

cooling (one of the variables in Bi/β) and elapsed time for three values of temperature ratio are presented in Figures 5 through 7. It is evident from these figures that β decreases to a minimum value at approximately $t^+ = 1$ and then increases with an increase in elapsed time. A conservative prediction of a "thin" skin thickness can be made through the use of a minimum β but this may be too restrictive if temperature distributions at times other than $t^+ = 1$ are desired. To fully utilize the results, the elapsed time should be specified. If temperature distributions at maximum skin temperatures are desired, this elapsed time to peak temperature may be determined from the results of the "thin" skin study (Figure C-2, Appendix C).

To illustrate how the elapsed time to the peak skin temperature is determined, consider the structure discussed above. From the conditions specified, calculate:

$$\tau = h_c \eta / \gamma C_p b$$

where: h_c = 25 Btu/hr ft^2 °F

η = 3/3600 hr

γ = 173 lb/ft^3 (density of 24S-T)

C_p = 0.23 Btu/lb °F (heat capacity of 24S-T)

b = 0.03/12 ft (thickness of skin)

Substitution of these values results in $\tau = 0.21$.

From Figure C-2, Appendix C, the elapsed time to the maximum skin temperature corresponding to $\tau = 0.21$ is 4.

With this elapsed time, $t^+ = 4$, in conjunction with $Bi/\beta = 0.014$ and a temperature ratio of 5%, β is found to be 1.15 (from Figure 5). From the definition of β, the skin thickness, b, can be calculated as follows:

$$\beta = b/\sqrt{a\eta} \qquad \text{so that}$$

$$b = \sqrt{a\eta}\ \beta$$

$$= 0.517 \text{ inch}$$

This result is interpreted to mean that from an elapsed time of 4 and longer,

skin thickness of 0.517 inch or less may be considered as "thin." This does not mean, however, that skin thickness less than 0.517 inch can not be considered to be "thin" for elapsed times less than 4. Thus, the skin thickness, 0.03 inch, of the structure may be considered "thin" at least from an elapsed time, t^*, of 4 on.

Set II, Figure 8.

The curves in Figure 8 were constructed from Figures 5 through 7 by plotting the minimum values of β as a function of Bi/β with the temperature ratio as a parameter. It may be noted from these curves that for a given material and time to peak input, increased convection results in decreased skin thicknesses that may be considered "thin". In contrast with skin thicknesses determined from Figures 5-7, those obtained from Figure 8 may be considered "thin" at any elapsed time.

For the illustrative example considered previously, Bi/β was computed to be 0.014. Using this value of Bi/β and the 5% temperature ratio curve of Figure 8, β is found to be 0.405. The skin thickness for this value of β is 0.182 inches. In this example, 0.182 inch skin thickness or less may be treated as "thin" through the entire time range.

Set III, Figures 9 and 10.

Curves in Figures 9 and 10 were obtained by using the minimum values of β in Figure 8 for temperature ratios of 5% and 10% respectively, in conjunction with the expression relating skin thickness and β_{min}. This expression written as

$$b = \beta_{min}\sqrt{a\eta}$$

was plotted in Figures 9 and 10 by using time to peak input, η, as the independent variable and diffusivity, a, as a parameter.

In the illustrative example, the time to peak input was given as 3/3600 hr. and the structure was constructed of aluminum whose diffusivity, a, is 1.68 ft^2/hr. From Figure 8, the skin thickness is found to be 0.135 inches. This skin thickness or less may be treated as "thin" through the entire time range for the conditions specified in the example.

Set IV, Figure 11.

This figure contains only a single curve relating β_{min} as a function of percent temperature ratio. These minimum values of β in the range of $0 < Bi/\beta < 2$ were obtained from Figure 8. This single curve is used in conjunction with equation 30,

$$b = \beta_{min}\sqrt{a\eta}$$

which contains the time to peak input, the thermal diffusivity of the material, and β_{min} which is found from Figure 11 by specifying the percent temperature ratio.

It is evident that the skin thicknesses calculated for each set differ considerably. For the illustrative example, the skin thicknesses varied from 0.135 inches to 0.517 inches. Note that the skin thickness (.03 in) of the example is much smaller than the smallest predicted thin skin. Thus, temperature distribution for this structure may be determined by using the "thin" plate theory.

SECTION V
CONCLUSIONS

The following conclusions may be drawn from the results of this investigation.

1. In general, a larger thermal diffusivity resulted in a larger minimum "thin" skin thickness.
2. In general, a longer reference time resulted in a larger minimum "thin" skin thickness.
3. A larger convective cooling resulted in a smaller minimum "thin" skin thickness. (The effect of convective cooling on the minimum skin thickness is small.)
4. For the range, $0 < Bi/\beta < 2$, the minimum skin thickness occurs at approximately the peak point of input function (at $t^+ = 1$).

BIBLIOGRAPHY

1. Coulbert, C.D., MacInnes, W.F., Ishimoto, T., Bussell, B., Ambrosio, A., *Temperature Response of Infinite Flat Plates and Slabs to Heat Inputs of Short Duration at One Surface,* Air Force Contract AF 33(038)-14381, University of California, Los Angeles, April 1951.

2. Ambrosio, A., Bussell, B., MacInnes, W.F., *Temperature Distributions in a Typical Aircraft Structure due to Transient External Heating,* Volume I, T-33 Airplane, WADC TR 52-216, Department of Engineering, University of California, Los Angeles, April 1953.

3. Ambrosio, A., and Ishimoto, T., *Temperature Distributions in a Typical Aircraft Structure due to Transient External Heating, Volume II, B-36 Airplane,* WADC TR 52-216, Department of Engineering, University of California, Los Angeles, August 1953 **(Confidential).**

4. Ambrosio, A., and Ishimoto, T., *Analytical Studies of Aircraft Structures Exposed to Transient External Heating, Volume I, Thermal Response of a "Thin" Plate under the Influence of a Constant Temperature Edge,* WADC TR 54-579, Department of Engineering, University of California, Los Angeles, May 1954.

5. Rubesin, M.W., *The Effect of an Arbitrary Surface Temperature Variation Along a Flat Plate on the Convective Heat Transfer in an Incompressible Turbulent Boundary Layer,* NACA TN 2345, 1951.

6. Tribus, M. and Klein, J., *Forced Convection from Nonisothermal Surfaces,* Heat Transfer Symposium, Engineering Research Institute, University of Michigan, 1953.

7. Churchill, Ruel V., *Modern Operational Mathematics in Engineering,* McGraw-Hill, 1944.

8. Hudson, R., *The Engineers Manual,* Wiley and Sons, London, 1947.

9. *Republic Titanium and Titanium Alloys,* Republic Steel Corporation, 1952.

10. Gmelin, L., *Handbuch Der Anorganishen Chemie,* Stechert and Co., New York.

APPENDIX A
POLES OF THE TRANSFORMED SOLUTION

The Laplace transformed solution for the temperature distribution in a finite plate (equation 13) written as a product of the transformed input function, $q^*(s)/I = f_1(s)$, and the transformed system function

$$\frac{\cosh\sqrt{s}\,\beta y}{\frac{\sqrt{s}}{\beta}\sinh\sqrt{s}\,\beta + \tau\cosh\sqrt{s}\,\beta} = f_2(s)$$

is inverted by the method of residues. Because $f_1(t) = \mathcal{L}^{-1}\{f_1(s)\}$ ($\mathcal{L}^{-1}$, notation for inversion) is a general expression that is convoluted with the system function, only the poles of the latter remain to be found.

These poles satisfy the denominator of $f_2(s)$ set to zero. This equation is expressed as,

$$\frac{\sqrt{s}}{\beta}\sinh\sqrt{s}\,\beta + \tau\cosh\sqrt{s}\,\beta = 0 \qquad \text{(A-1)}$$

Although, s, is a complex variable of Laplace transformation, the poles all lie on the negative real axis. This is shown as follows:

Let: $\sqrt{s}\,\beta = \alpha$

$= U + iV$

and because $\tau\beta^2 = Bi$ (Bi is Biot's Modulus), equation (A-1) becomes,

$$(U + iV)\sinh(U+iV) + Bi\cosh(U+iV) = 0 \qquad \text{(A-2)}$$

Expanding equation (A-2) into its real and imaginary parts and equating the real and imaginary parts of (A-2) to zero results in:

Real Part

$$U(\sinh U)\cos V - V(\cosh U)\sin V + Bi\ \cosh U(\cos V) = 0 \qquad \text{(A-3a)}$$

Imaginary Part

$$V(\sinh U)\cos V + U(\cosh U)\sin V + Bi\ \sinh U(\sin V) = 0 \qquad \text{(A-3b)}$$

Values of U and V which satisfy equations (A-3a) and (A-3b) necessarily satisfy equation (A-1). By rearranging the terms, equations (A-3) may also be written as,

$$\tanh U = \frac{1}{U}\,\frac{V\sin V - Bi\cos V}{\cos V} = \frac{1}{U}\,(V\tan V - Bi) \qquad \text{(A-4a)}$$

$$\tanh U = -\frac{U\sin V}{V\cos V + Bi\sin V} = -\frac{U}{V\cot V + Bi} \qquad \text{(A-4b)}$$

Equations (A-4) are identical for positive and negative V's and U's because the functions $V\tan V$, $V\cot V$, $U\tanh U$, and $\tanh U/U$ are all even functions. The values of U that satisfy equations (A-4a) and (A-4b) can be found most simply by plotting the left and right hand terms of both equations as functions of U.

Consider equation (A-4b)

For the range of V,

$$2n\pi \le V \le (2n + 1/2)\pi$$

$$(2n + 1)\pi \le V \le (2n + 3/2)\pi$$

the two functions only have one point of intersection for all positive values of Bi. This occurs at the origin as shown in Figure A-1.

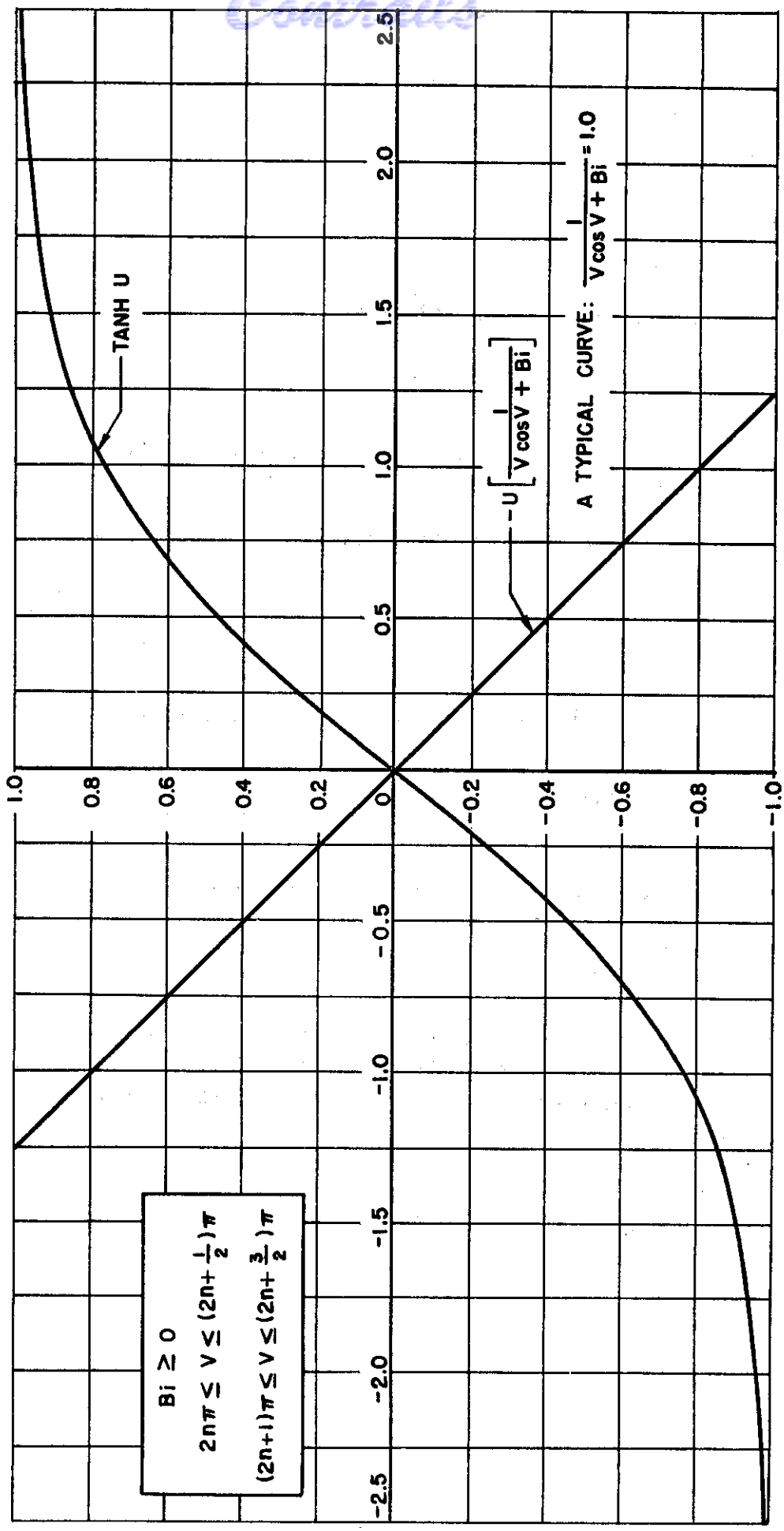

FIGURE A-1 FIRST OF TWO GRAPHS SHOWING POLES ARE IMAGINARY

Consider equation (A-4a)

For the range of V,

$$(2n + 1/2)\pi \leq V \leq (2n + 1)\pi$$

$$(2n + 3/2)\pi \leq V \leq (2n + 1)\pi$$

there are no values of U which will satisfy equation (A-4a). This is shown graphically in Figure A-2.

Hence equation (A-2) can be satisfied only if U is zero. This means that

$$\alpha = iV = \sqrt{s}\,\beta \tag{A-5}$$

so that the poles of the system function are all negative:

$$s = -(V^2/\beta^2) \tag{A-6}$$

These values of V are the roots of the equation

$$\tan V = Bi/V,$$

which was found by substituting equation (A-5) into (A-1). The roots, that are approximated graphically as shown in Figure A-3, occur within a periodic interval and are known as eigenvalues. Note only the positive values have Been considered.

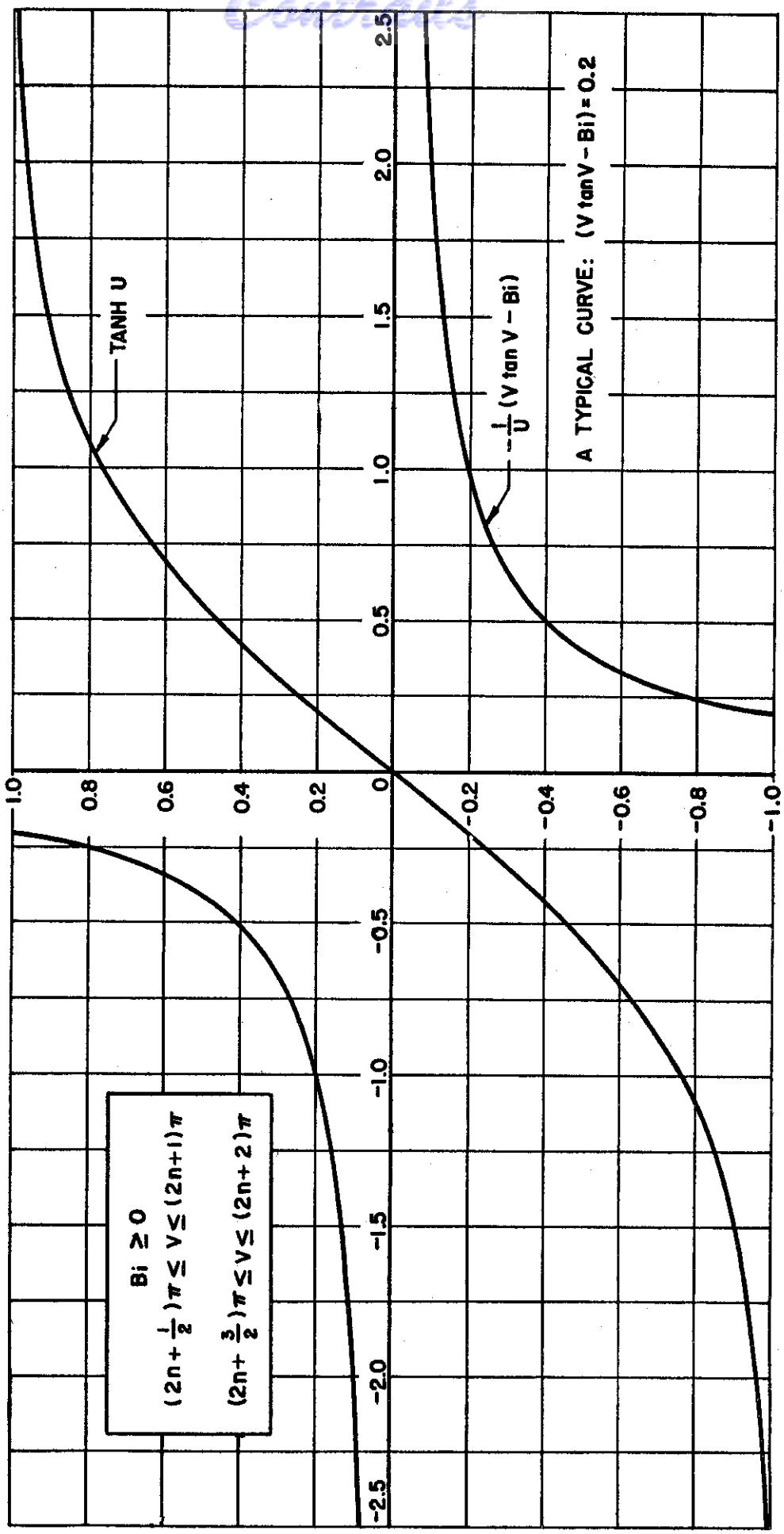

FIGURE A-2 SECOND OF TWO GRAPHS SHOWING POLES ARE IMAGINARY

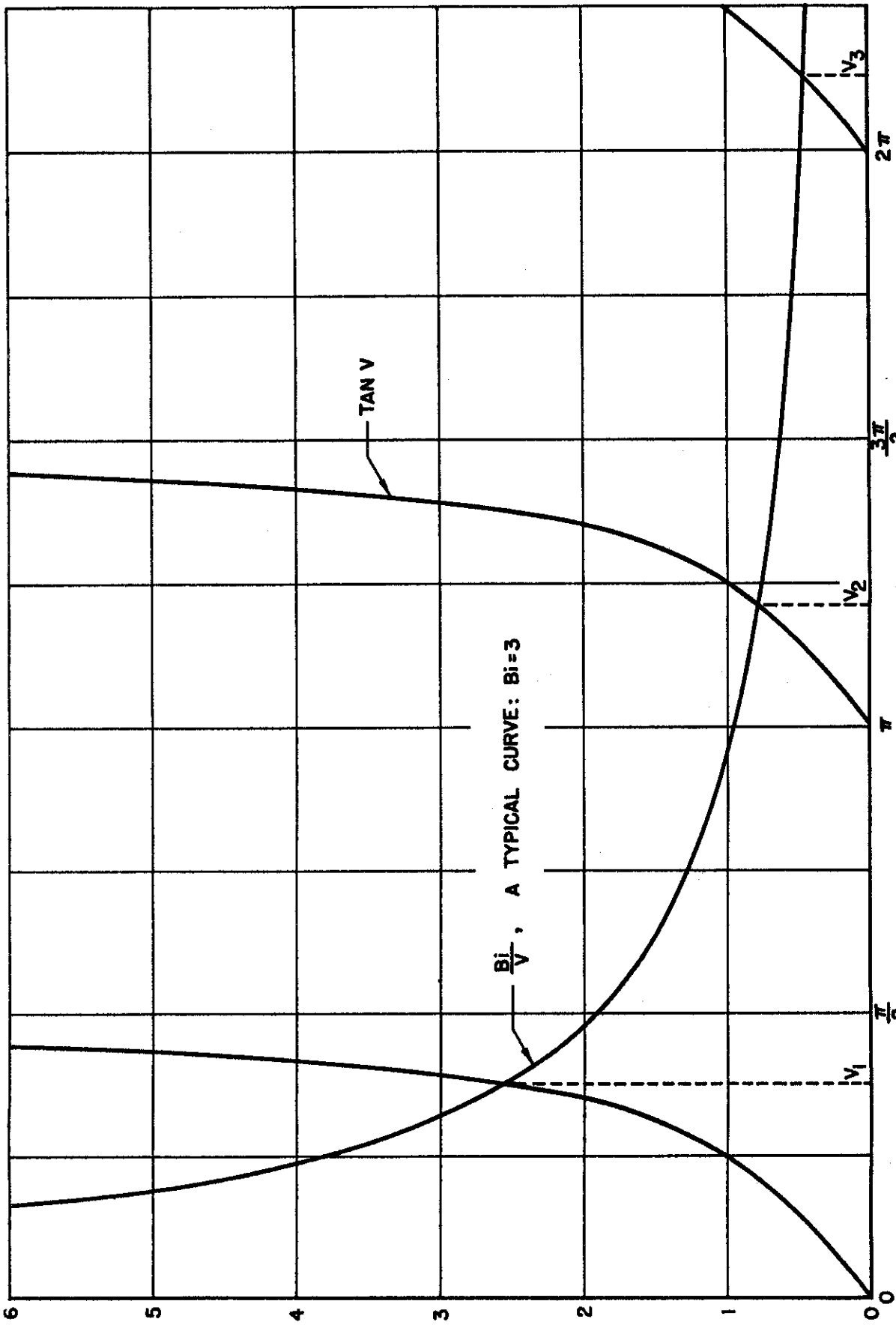

FIGURE A-3 A PLOT OF TAN V = $\frac{Bi}{V}$, (Bi=3)

APPENDIX B

A METHOD OF EVALUATING THE TEMPERATURE SOLUTION

The expression for the temperature response of a finite plate is a convolution integral containing a product of the forcing function and the sum of an infinite series.

$$T^+(Y, t^+) = 2 \int_0^{t^+} \frac{q^+(\lambda)}{I} \sum_{n=1}^{\infty} \frac{(\cos V_n Y) \exp\left[-\frac{V_n^2}{\beta^2}(t^+ - \lambda)\right]}{\cos V_n \left[1 + \frac{Bi}{V_n^2}(1 + Bi)\right]} d\lambda \qquad \text{(B-1)}$$

Assuming that the convolution integral of equation (B-1) can be replaced by a sum of convolution integrals, each containing the product of the forcing function and a term of the series, the temperature expression becomes,

$$T^+(Y, t^+) = 2 \sum_{n=1}^{\infty} \frac{\cos V_n Y}{\cos V_n \left[1 + \frac{Bi}{V_n^2}(1 + Bi)\right]} \int_0^{t^+} \frac{q^+(\lambda)}{I} \exp\left[-\frac{V_n^2}{\beta^2}(t^+ - \lambda)\right] d\lambda \qquad \text{(B-2)}$$

Each term of the series (B-2) is independent of the other terms in the series. This means that the temperature response of the plate can be considered to be a sum of finite temperature changes, $\Delta T_n^+ (n = 1,2,3 \ldots.)$, each one represented by a convolution integral of the type,

$$\Delta T_n^+ = 2 \frac{\cos V_n Y}{\cos V_n \left[1 + \frac{Bi}{V_n^2}(1 + Bi)\right]} \int_0^{t^+} \frac{q^+(\lambda)}{I} \exp\left[-\frac{V_n^2}{\beta^2}(t^+ - \lambda)\right] d\lambda \qquad \text{(B-3)}$$

That is:

$$T^+ = \Delta T_1^+ + \Delta T_2^+ + \cdots + \Delta T_n^+ + \cdots = \sum_{n=1}^{\infty} \Delta T_n^+ \qquad \text{(B-4)}$$

Consider a single convolution integral associated with a corresponding ΔT_n^+ (equation B-3) and divide this equation through by

$$f_n(V_n, Y, Bi) = \frac{\cos V_n Y}{\cos V_n \left[1 + \frac{Bi}{V_n^2}(1 + Bi)\right]}$$

Thus,

$$F_n \equiv \frac{\Delta T_n^+}{f_n(V_n, Y, Bi)} = \int_0^{t^+} \frac{q^+(\lambda)}{I} \exp\left[-\frac{V_n^2}{\beta^2}(t^+ - \lambda)\right] d\lambda \qquad \text{(B-5)}$$

But the solution to a "thin" plate system[4] heated by the same input, $q^+(t^+)/I$ is identical to the right-hand side of equation (B-5) if V_n^2/β^2 is replaced by τ, i.e.,

$$T_{F.P.}^+ = \int_0^{t^+} \frac{q^+(\lambda)}{I} \exp\left[-\tau(t^+ - \lambda)\right] d\lambda \qquad \text{(B-6)}$$

Thus, F_n may be obtained by using the solution for $T_{F.P.}^+$. A sketch of the "thin" plate system and typical solution curves are shown in Figure B-1.

The method used to evaluate ΔT_n^+ was the following:

(1) Compute V_n^2/β^2

(2) Determine F_n from the curves of $T_{F.P.}^+$ versus τ at the desired t^+, using $\tau = V_n^2/\beta^2$

(3) Compute $f_n(V_n, Y, Bi)$ from $f_n = \frac{2 \cos V_n Y}{\cos V_n \left[1 + \frac{Bi}{V_n^2}(1 + Bi)\right]}$

This function is completely defined for a given Y and Bi.

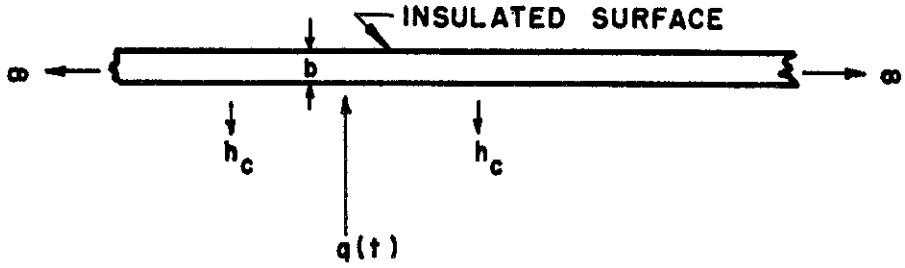

DIFFERENTIAL EQUATION: $\frac{dT^+_{T.P.}}{dt^+} = \frac{q^+(t^+)}{I} - \tau T^+_{T.P.}$

SOLUTION: $T^+_{T.P.} = \int_0^{t^+} \frac{q^+(\lambda)}{I} \text{ EXP } [-\tau(t^+ - \lambda)]\, d\lambda$

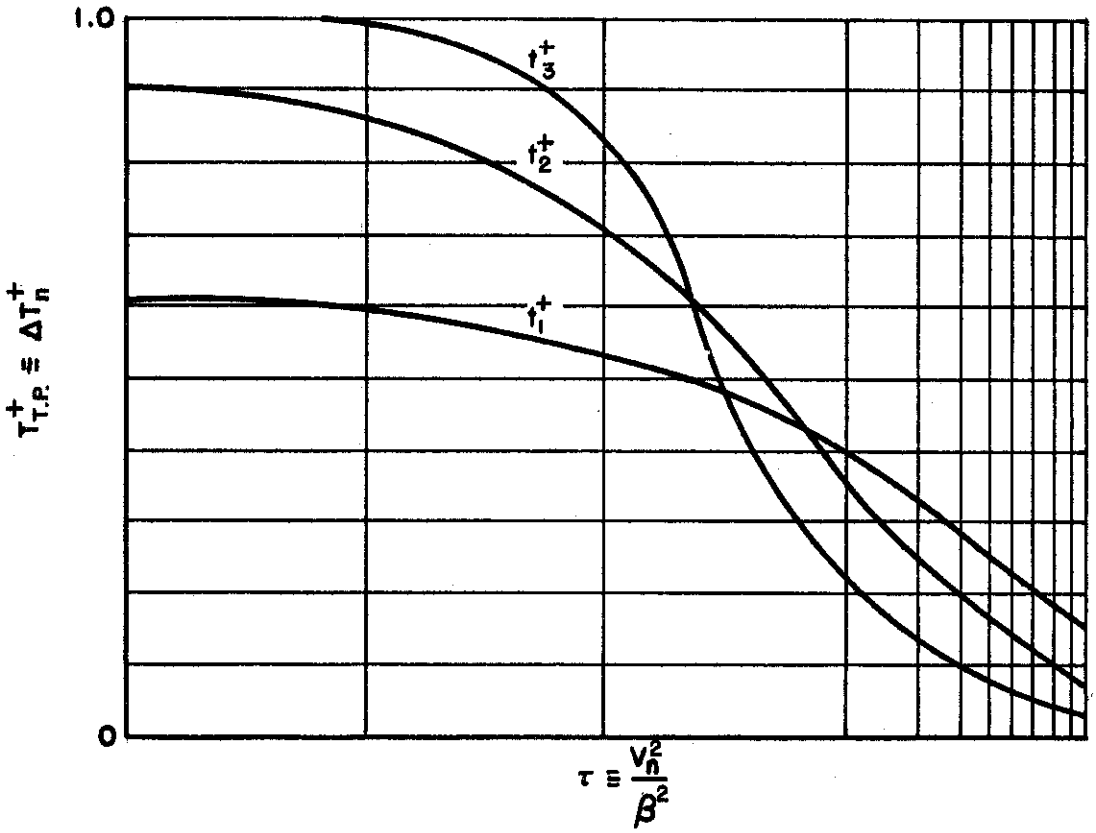

FIGURE B-1 "THIN" PLATE SYSTEM WITH A TYPICAL GRAPHICAL REPRESENTATION OF SOLUTION

(4) Compute ΔT_n^+ from the relation,

$$\Delta T_n^+ = F_n f_n(\nabla_n, Y, Bi)$$

The temperature, T^+, is found by summing the individual terms, ΔT_n^+.

$$T^+ = \sum_{n=1}^{\infty} \Delta T_n^+ \qquad \text{(B-4)}$$

For large ∇_n^2/β^2 ($\nabla_n^2/\beta^2 > 100$), the evaluation of $T^+_{n(F.P.)}$ can be simplified considerably by reducing the solution to the differential equation (B-1) describing a "thin" isolated skin region,

$$T^+_{F.P.} = \int_0^{t^+} \frac{q^+(\lambda)}{I} \exp\left[-\tau(t^+ - \lambda)\right] d\lambda \qquad \text{(B-6,}$$

to the expression

$$T^+_{F.P.} = \frac{1}{\tau} \frac{q^+(t^+)}{I} \qquad \text{(B-7)}$$

That is, for large $\nabla_n^2/\beta^2 \equiv \tau$,

$$T^+_{F.P.} = \int_0^{t^+} \frac{q^+(\lambda)}{I} \exp\left[-\tau(t^+ - \lambda)\right] d\lambda \cong \frac{q^+(t^+)}{I} \int_0^{t^+} \exp\left[-\tau(t^+ - \lambda)\right] d\lambda$$

$$\cong \frac{1}{\tau} \frac{q^+(t^+)}{I}$$

A physical interpretation is that the heat storage by the skin is negligible as compared to convective cooling from the skin.

APPENDIX C
ISOLATED "THIN" PLATE SOLUTION

The thermal response of an isolated "thin" plate that is sketched in Appendix B was discussed in reference (4). The differential equation of the system is,

$$\frac{d\,T^{+}_{T.P.}}{dt^{+}} = \frac{q^{+}(t^{+})}{I} - \tau\, T^{+}_{T.P.} \qquad \text{(C-1)}$$

and the solution to this expression is written as,

$$T^{+}_{T.P.} = \int_{0}^{t^{+}} \frac{q^{+}(\lambda)}{I}\, exp\left[-\tau\,(t^{+}-\lambda)\right] d\lambda \qquad \text{(C-2)}$$

The notation in these expressions are consistent with those found in the present report. A series of curves, $T^{+}_{T.P.}$ vs. t^{+}, with τ as a parameter result from the evaluation of the integral in equation (C-2). For the present study, only those conditions at maximum temperature rises are of interest. Plots of $T^{+}_{m(T.P.)}$ vs. τ and $t^{+}_{T^{+}_{m(T.P.)}}$ vs. τ are presented in Figures C-1 and C-2, respectively.

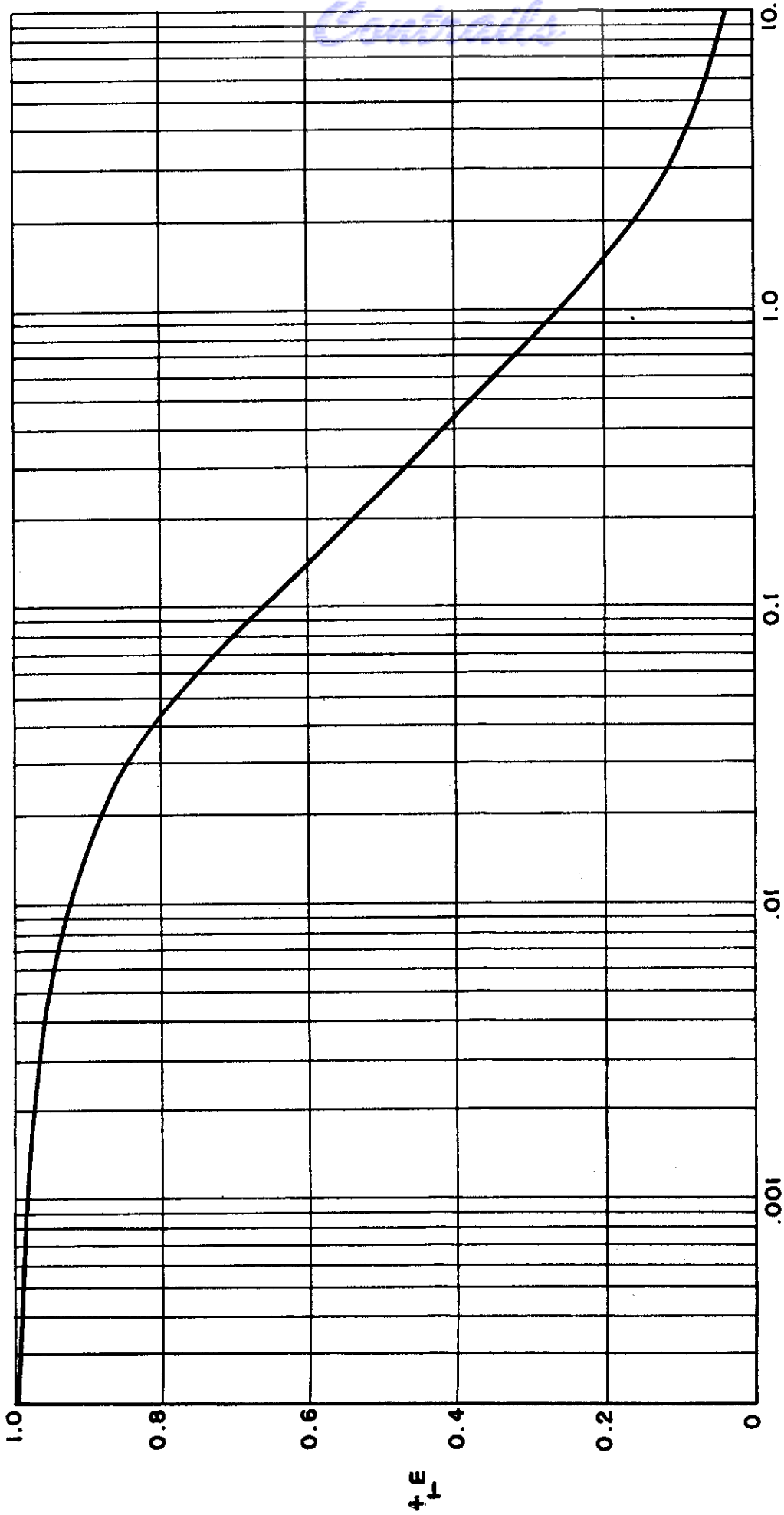

$$\tau = \frac{h_c \eta}{\gamma C_p b}$$

FIGURE C-1 MAXIMUM "THIN" SKIN TEMPERATURE RISE

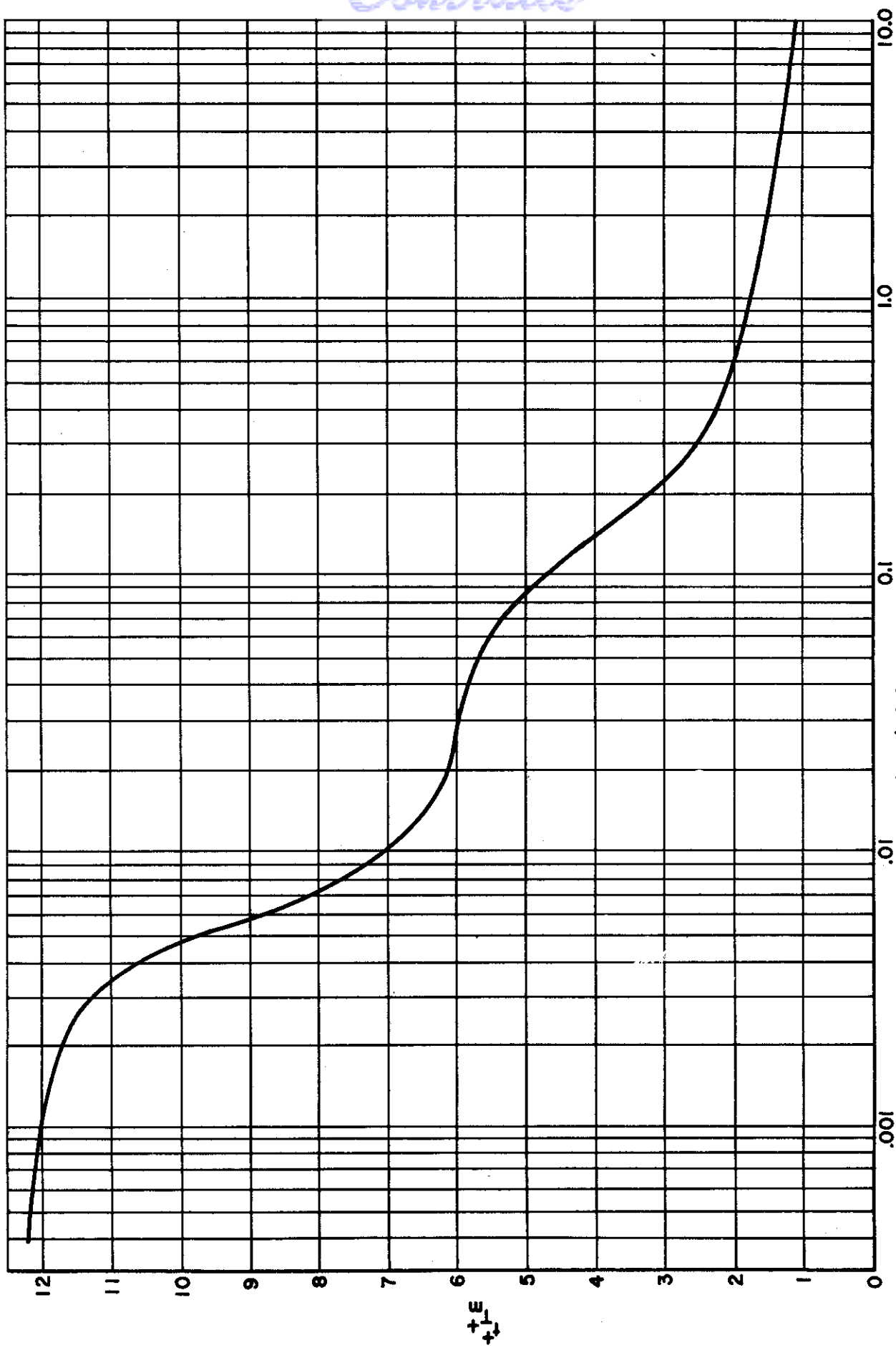

FIGURE C-2 TIME TO PEAK "THIN" SKIN TEMPERATURE RISE

DISTRIBUTION LIST

SECTION I

Addressee	Copies
Commander, Wright Air Development Center Wright-Patterson AFB, Ohio Attn: WCLS	2
Commander, Wright Air Development Center Wright-Patterson AFB, Ohio Attn: WCOSI-4	3
Commander, Wright Air Development Center Wright-Patterson AFB, Ohio Attn: Lt. Col. S.W. Bowman, WCOES	2
Director, Armed Services Technical Information Agency Document Services Center Knott Building, Dayton 2, Ohio Attn: DSC-SA	5

SECTION II

Chief, Bureau of Aeronautics Department of the Navy Attn: Mr. Robert F. Speaker, Ad-11 Washington 25, D.C.	2
Director U.S. Naval Research Laboratory Washington 25, D.C.	1
Chief, Bureau of Ordnance Department of the Navy Washington 25, D.C.	1
Director, The Material Laboratory New York Naval Shipyard Attn: J. M. McGreevy Brooklyn 1, New York	1
Chief of Naval Operations (OP-55) Navy Department Washington 25, C.C.	1
Commander, Operational Development Force U.S. Naval Base, Norfolk 11, Va.	1
Commanding Officer Air Development Squadron Five, VX5 U.S. Naval Air Station Moffett Field, California	1
Commanding Officer Naval Air Special Weapons Facility Kirtland Air Force Base, New Mexico	1
Commanding General Aberdeen Proving Ground, Maryland Attn: Mr. H.K. Weiss	1
Deputy Chief of Staff, Operations Hq USAF, Attn: Assistant for Atomic Energy Washington 25, D.C.	1
Director of Operations, Hq USAF Washington 25, D.C.	1
Chief of Naval Research Code 219- Rm 1807, Bldg T-3 Attn: RD Control Officer Washington 25, D.C.	1
Dr. Edward O. Hulbert Naval Research Laboratory Washington 25, D.C.	1
Commanding Officer U.S. Naval Radiological Defense Lab. Attn: Dr. Andrew Guthrie San Francisco 24, California	2
Commander U.S. Naval Air Development Center Johnsville, Pa.	1
Chief of Naval Operations (OP-36) Navy Department Washington 25, D.C.	1
Commanding Officer, Naval Air Test Center Patuxent River, Md.	1
Commanding Officer Air Development Squadron Three, VX3 U.S. Naval Air Station Moffett Field, California	1
Office of Operational Research Johns Hopkins University Fort Leslie J. McNair Attn: Brig. Gen. L.O. Flory Washington 25, D.C.	1
Chief of Research and Development Department of the Army Washington 25, D.C.	1
Deputy Chief of Staff Operations Hq USAF Attn: Dr. J.C. Mouzon, Rm 5D-870 Washington 25, D.C.	1

Addressee	Copies
Director of Operations Hq USAF Attn: Operations Analysis Washington 25, D.C.	1
Commander, Strategic Air Command Attn: Chief Operations Analysis Offutt Air Force Base, Nebraska	1
Commander, Tactical Air Command Attn: Chief, Operations Analysis Section Langley Air Force Base, Virginia	1
Commander, Air Defense Command Attn: ADMAR-2, Ent Air Force Base Colorado	1
Commander, Air Research and Development Command Attn: RDTDA, P.O. Box 1395 Baltimore 3, Md.	3
Commander, Air Research and Development Command Attn: RDGT, Col. D'Ettore P.O. Box 1395 Baltimore 3, Md.	1
Director, Air University Library ATTN: CR-5755 Maxwell Air Force Base, Ala.	1
Deputy Chief of Staff, Development, Hq USAF Attn: Lt. General D. Putt Washington 25, D.C.	1
Deputy Chief of Staff Development, Hq USAF Attn: Major Beavers Washington 25, D.C.	1
Deputy Chief of Staff Development, Hq, USAF Attn: Development Planning Washington 25, D.C.	2
Deputy Chief of Staff Development, Hq USAF Attn: Director of Research and Development Strategic Air Group Washington 25, D.C.	1
Deputy Chief of Staff Development, Hq, USAF Attn: Director of Research and Development Aeronautics Division Washington 25, D.C.	1
Director of Intelligence Hq USAF Washington 25, D.C.	1
Director of Intelligence Hq USAF Attn: Physical Vulnerability Division Washington 25, D.C.	1
Commander Air Force Special Weapons Center Attn: AF Atomic Energy Library Kirtland Air Force Base, New Mexico	3
Executive Secretary Weapons Systems Evaluation Group Office of the Secretary of Defense The Pentagon Washington 25, D.C.	1
Director of Military Application U.S. Atomic Energy Commission 1901 Constitution Avenue, N.W. Washington 25, D.C.	1
Director, Division of Research U.S. Atomic Energy Commission Washington 25, D.C.	1
Chief, Armed Forces Special Weapons Project Attn: SWPTI-2 Washington 25, D.C.	1
Headquarters Field Command Armed Forces Special Weapons Project Technical Training Group Library Attn: Miss E. Pauline Dunlavy, Librarian Sandia Base, New Mexico	2
Commander Air Force Cambridge Research Center 230 Albany Street Cambridge 39, Mass. Attn: Robert Chapman Geophysics Research Directorate	1
Army Field Forces Department of the Army Directorate of Special Weapons Development Fort Bliss, Texas	1
Chief, Bureau of Ordnance Department of the Navy Attn: KE-9, Washington 25, D.C.	1
Bureau of Aeronautics Washington 25, D.C. Attn: Ralph Zirkino, RS-5	1

SECTION III

Addressee	Copies
Dr. Alvin C. Graves J-1 Division Los Alamos Scientific Laboratory P.O. Box 1663 Los Alamos, New Mexico	2
Dr. Harold Agnew, Director's Office Los Alamos Scientific Laboratory P.O. Box 1663 Los Alamos, New Mexico	1
Director, NACA Attn: Richard Rhode 1512 H Street, N.W. Washington 25, D.C.	1

SECTION IV

Addressee	Copies
University of California Department of Engineering Engineering Research Attn: Prof. Walter C. Hurty Los Angeles 24, California	40
Massachusetts Institute of Technology Department of Aeronautical Engineering Aeroelastic and Structures Research Lab. Attn: Mr. J.C. Loria Cambridge 39, Mass.	1
Allied Research Associates, Inc. Attn: Mr. Lawrence Levy, President 43 Leon Street Boston 15, Mass.	1
Massachusetts Institute of Technology Department of Mechanical Engineering Attn: Prof. H.C. Hottel Cambridge 39, Mass.	1
Rand Corporation (Thru: WCOSI) Attn: Dr. E.H. Plesset 1700 Main Street Santa Monica, California	2
Vitro Corporation of America Attn: Dr. C.T. Molloy P.O. Box 146 Verona, New Jersey	1
Bell Aircraft Corporation Attn: Chief Engineer Niagara Falls, New York	1
Boeing Airplane Company Attn: E. Wells, Chief Engineer 200 W. Michigan Avenue Seattle 14, Washington	2
Chance Vought Aircraft, Inc. Attn: Chief Engineer Dallas, Texas	1
Consolidated Vultee Aircraft Corporation Attn: R. H. Widmer, Chief Engineer Fort Worth Division Fort Worth, Texas	1
Consolidated Vultee Aircraft Corporation Attn: Chief Engineer, San Diego Division San Diego 12, California	1
Douglas Aircraft Company, Inc. Attn: Charles Strang 300 Ocean Park Blvd. Santa Monica, California	1
Douglas Aircraft Company, Inc. Attn: J.C. Buckwalter, Chief Engineer 3855 Lakewood Blvd. Long Beach, California	1
Grumman Aircraft Engineering Company Attn: Chief Engineer, Bethpage Long Island, New York	1
Lockheed Aircraft Corporation Factory A Attn: Jerome C. McBrearty P.O. Box 71 Burbank, California	1
Glenn L. Martin Company Attn: Chief Engineer Baltimore 3, Md.	1
McDonnell Aircraft Corporation Attn: Chief Engineer P.O. Box 516 Municipal Airport St. Louis, Mo.	1
North American Aviation, Inc. Attn: R.L. Schleicher Municipal Airport Los Angeles, California	1

Addressee	Copies
Northrop Aircraft, Inc. Attn: Miss M.J. Sommer, Librarian Northrop Field, Hawthorne, California	1
Republic Aviation Corporation Attn: Chief Engineer Farmingdale Long Island, New York	1
Cook Research Laboratories Division of Cook Electric Company 8100 Monticello Avenue Skokie, Ill.	1
Johns Hopkins University Operations Research Office 6410 Connecticut Ave. Chevy Chase, Md.	1
University of Dayton Division of Research Attn: Dr. K.C. Schraut Dayton 3, Ohio	1
Assessment Group c/o Applied Physics Laboratory Johns Hopkins University Attn: Technical Reports Office Silver Spring, Md.	1
Boeing Airplane Co. Wichita Division Attn: Messrs B. Hodges and K.K. Holtby Wichita, Kansas	1
California Institute of Technology Guggenheim Aeronautical Laboratory Attn: Prof. E.E. Sechler Pasadena, California	1
Columbia University Department of Civil Engineering Attn: Dr. Bruno A. Boley New York 27, New York	1
New York University College of Engineering Dept. of Mechanical Engineering Attn: Dr. Frederick Landis University Heights New York 53, N.Y.	1
New York University College of Engineering Dept. of Aeronautical Engineering Attn: Prof. Frederick Teichman University Heights New York 53, New York	1